

## Reviewer 1

### *Summary:*

*The authors collected samples of functionalized organic compounds from a wildfire using an aircraft platform. Particles were collected on filters and sampled using LC and GC techniques offline, while gas phase compounds were collected in adsorbent tubes and sampled primarily using the LC method offline. The authors illustrate the importance of sulfide compounds, concluding that sulfides are formed through secondary chemistry and are a major contributor to CHONS compounds after plume aging. They discuss possible sources of these sulfur compounds. The measurements and analysis are quite interesting, and definitely of interest to others researching organic compounds (particularly lower volatility gases and particulate speciation). I have one major issue with how the authors quote numbers for relative contributions of sulfide and CHONS in the abstract, rather than using (dilution corrected) absolute concentrations to really prove that secondary formation is occurring. The data supporting abstract-level conclusions needs to be presented in the main paper, rather than the SI figures. This issue can be resolved through reorganization, and after addressing that along with my other comments, I would recommend for publication.*

We thank the reviewer for their supportive comments. We modified our figure presentation and our discussion of the data in the abstract and manuscript to address both the absolute and relative contributions from CHONS and sulfide species. We discuss our edits in detail in the line-by-line responses below.

### *Specific Comments:*

*Abstract, Sect 3.1, 3.2, etc.: In several places in the main text and figs including the abstract, Sects. 3.1 and 3.2, you present data by relative abundance of each screen. You present that the relative contribution of sulfides increases with plume age, and quote those numbers in the abstract in the context of saying sulfides are formed through secondary chemistry from S/IVOCs. However, the change in relative contribution alone could have several causes: sulfides could be being formed from chemistry in the plume (which is what you show with Fig. S6A with the CO-normalized plots), or sulfides could just be evaporating less than other functional groups and thus becoming relatively more important. Like I said, with Fig. S6A you show that the absolute concentration (when dilution corrected) is increasing, so there is some chemical formation, but you're not presenting your data or quoting the right numbers in the abstract to back up this conclusion. I believe this conclusion is really the main conclusion that you're trying to show with this work, and that's why you go on to a lot of discussion of possible secondary sources of sulfides in Sect. 3.5. But you're only showing it with an SI figure. This is a major issue with the organization of manuscript, in my opinion. And in the abstract, the quoted numbers seem potentially misleading to me. You present the numbers for relative increase (which on their own don't necessarily mean secondary formation, and might not quantitatively represent the amount of secondary formation), but the context is that sulfides are being formed through secondary chemistry. I think you need to be showing CO-normalized data in the main paper figs and quote those numbers in the abstract. As an imprecise use of data to back up conclusions in the abstract, I say it's a major issue, but it should be easy to resolve and it won't change your conclusions.*

We thank the reviewer for bringing up this important distinction. In Figure 1 and the associated discussion, we showed the contribution of CHONS and sulfide species in terms of their relative prevalence, to contrast changes in CHONS and sulfide contributions with other compound classes and functional groups in the observed complex mixture of emissions and transformation products. We agree that changes in relative contributions could be driven by a number of factors, such as chemical formation and different relative rates of evaporation that could vary between compound classes and functional groups. For this study, we were interested in looking at both the absolute formation of CHONS and sulfide species *and* the evolution of the overall complex mixture of compound classes/functional groups. As a result, we chose to include relative contributions of compound classes and functional groups in the main text, and in the interest of space, absolute contributions corrected for dilution (using carbon monoxide measurements) in the SI. We recognize that both ways of presenting results (i.e. as relative or absolute contributions) are valuable for different purposes. In both cases, the observed trends in CHONS and sulfide contributions were similar. Both approaches showed an overall growing contribution of CHONS and sulfides from screen 1 to 4, peaking at screen 4.

To address the reviewer's concern and provide more information the reader in the main text, we added an inset to Figure 1 that shows the absolute contributions of CHONS and sulfides with plume age (using dilution-corrected abundances). We added an inset rather than replacing the full figure because we did not want to lose the information presented in the current Figure 1A-C on the evolution of the complex mixture as a whole. In Figure 1's caption, we added an additional reference to the SI figures that show all compound classes and functional groups by absolute dilution-corrected abundance. We also note that we already show dilution corrected values for the gas-phase data in Figure 4. Also, in the abstract (lines 21-22 and 24-26) and in other instances where we reported the change in relative contribution of CHONS and sulfide species, we added a mention of their increase in dilution-corrected abundance. Finally, we included a note to the results section that draws attention to both methods of tabulation (lines 187-192).

*Line 180: Again, the increase in relative abundance of sulfides among CHONS species doesn't tell us whether sulfides are being formed, or if they're just evaporating/reacting more slowly than other functional groups. But the discussion here all assumes secondary formation. This is the same as my first comment, really.*

This concern is addressed above. At line 186-187, we added a sentence to show increases in absolute abundance (corrected for dilution using CO) to more strongly support the conclusion of CHONS formation. Similar additions were made when sulfides were discussed (lines 207-208).

*Fig. S5 and elsewhere: What is the difference between abundance and occurrence? I don't see it explained anywhere, so I don't know what point you're trying to make by showing plots of occurrence.*

The results shown in select SI figures tabulated by both abundance and occurrence are for comparison purposes only. The results tabulated by abundance are the ones discussed throughout the manuscript. However, due to uncertainty in ionization efficiency of individual multifunctional compounds within the complex mixture, we provide the reader with supporting data on the detailed distribution of compound classes, volatility ranges, and functional groups by occurrence as well (i.e. by number of compounds in each category). Trends in most cases were similar, suggesting that the interpretation of the abundance-weighted results was not substantially skewed by differences in ionization efficiency. This was originally discussed briefly at the end of SI Section S4. To address the reviewer's comment, we added a mention of the specific figures in the SI for which we showed both abundance-weighted and occurrence-based results for emphasis (SI lines 287-289). We also added a reference to Section S4 in the captions of the relevant figures, to draw attention to the discussion (Figures S5, S6, S8, S9).

*Line 195: How are you estimating the volatility of the compounds? It looks like you might be explaining in line 201 (and Fig. S8, S9 captions), but it would be good to give that detail in the methods section before you start discussing volatilities here.*

Thank you for the suggestion. We added a few sentences to the Materials and Methods section to discuss this for adsorbent tubes and filters (clarified lines 113-124, added lines 127-130 and lines 157-162).

*Line 82: Could you provide a little more info about the two-plume structure of the fire? Was it two spots of active burning/smoldering, and if so how close were they, or was it one spot that evolved two plumes with different ages? Mainly, I just want to know if both plumes in a given screen were sampled at approximately the same age. Maybe you could indicate an approximate location of the start of the second plume in Fig S1.*

Based on analyses of satellite imagery and ground meteorological measurements, the NP was likely from the same source as the South Plume (SP). The NP likely occurred due to a switch in wind direction just prior to sampling. This means that the NP may be slightly older than the SP—we estimate this age difference to be <30 minutes, so they are roughly the same age. We added a brief mention of the ages of the plumes to the caption of Figure S1. Because the source of the NP was not identified via satellite imagery, it is not included explicitly in Figure S1 (this is mentioned in the caption).

*Line 87: What were the altitudes sampled in each screen?*

The average altitude of samples varied ~650-1650 m for adsorbent tubes (collected on distinct low and high altitude passes through the plume), and ~900-1600 m for filters (one filter per screen). Average altitudes were originally shown in Table S1, and we

added a reference to this table at line 90 to ensure that this information is readily found by readers.

*Line 214: There are a lot of acronyms and methods involved in your analysis (not a criticism, just an observation!), so it can be a little tricky to follow that you're switching now from discussing the particle phase that was sampled via filters to discussing the gas phase sampled via adsorbent tubes. I'd recommend just adding a quick note here to say this more explicitly, that in order to try to understand the particle phase filter measurements presented earlier, you're now doing targeted analysis of the gas phase sampled via adsorbent tubes.*

We edited this sentence to make the transition clearer to readers (line 246-248).

*Line 300: Could you discuss whether or not there are any sulfur-containing compounds included in any fire suppressant materials that could have been deposited on this fire?*

Smoke from this fire was sampled when the fire was less than 1 hour old and there had been no prior active fire suppression activities. Fire suppressant from past applications could have deposited on forest surfaces and re-volatilized, though historically, fire suppressants are not heavily used this region due to the abundance of lakes in the area. Also, this region uses water almost exclusively as a fire retardant. While it is possible that non-water fire suppressants were applied historically, the exact type and quantity are uncertain. It appears that one of the most commonly used fire suppressants in Canada today contains ammonium phosphate salts, sometimes with sulfate-containing salts mixed in. The exact composition of a few example fire suppressants that we searched for were proprietary, so the contribution of sulfate salts is unknown, but likely minor compared to that of phosphate salts. The contribution of any sulfur-containing compounds from fire suppressants to the observed gas/particle-phase species is therefore expected to be minor or negligible (if 100% water was used). We added a sentence to briefly mention fire suppressants at lines 366-368.

*Sects. 3.4 and 3.5: Both of these sections are entirely 'discussion' of what could be explaining your data, and not presentation of your 'results'. Thus, they don't need to have their own sections under your 'results and discussion' header. You should either move them up into the previous sections where you actually present the results you're discussing, or change Sect. 3 to just 'Results' and have Sect. 4 be "Discussion" including these two sections (and make Conclusions be Sect. 5).*

Thank you for the suggestion. We turned section 3 into "Results", moved 3.4-3.5 to "Discussion" (now 4.1-4.2), and adjusted the "Conclusions" to become section 5.

*SI line 75: extra s in VOCs*

This has been corrected.

*Fig. S9: Should include a legend for screens 1-5, as in Fig S5, for completeness*

We added a legend to panel A.

*Section S5: This whole section is great! Provides really nice context for interpreting all of the measurements you present throughout the manuscript. I'd advocate for moving Sect. S5 to the end of the main paper methods section.*

We thank the reviewer for the supportive comment. We felt that the comprehensive discussion of the differences between LC-ESI and GC-APCI methods was better suited to the SI, so that we could include several numerical details that described the types of compounds accessible with each technique without bogging down the reader with too many supplemental details in the main text. However, we have taken the reviewer's recommendation and added a short paragraph to the end of the Materials and Methods section that introduces the longer discussion in the SI (lines 148-156).

*Fig 1A along with Section S5: So Fig. 1A is really showing the relative abundance of the part of OA that could be sampled using the LC-ESI-MS method. You say LC is better for larger, more polar, more functionalized, less volatile compounds. How could this be biasing your percentages in Fig. 1A? E.g., maybe the sulfur compounds tend to be lower volatility and better sampled, while some less oxidized, less polar CHO compounds are poorly sampled? Some discussion would be useful, especially if you bring Sect. S5 to the main paper.*

The LC-ESI methods used in this work are better suited for detecting more functionalized and polar compounds present in the OA sampled on PTFE filters (IVOCs-SVOCs included). LC-ESI (using both positive and negative mode) is known to be effective for a wide range of species that contain at least one oxygen atom or one nitrogen atom (in addition to combinations of sulfur with oxygen and/or nitrogen, and combinations of all three heteroatoms), making it conducive for measurements of biomass burning emissions and transformation products. While these methods exclude CH and CHS species (i.e. fully reduced hydrocarbons and compounds containing reduced sulfur only), this was acknowledged in the text and filter samples were run on the GC-APCI to explore the contribution of CH and CHS species to the particle-phase. From the GC-APCI analysis of particle-phase samples, we observed a greater contribution from CHO species and relatively lower fractions of the other heteroatom-containing groups, including CHS. This is likely because these other heteroatom-containing species were less GC-amenable, and thus were lost during solvent extraction, lost to the GC inlet, or lost to the GC column during analysis.

Both LC-ESI and GC-APCI methods have column transmission and ionization strengths and weaknesses for different classes of compounds. The focus of this manuscript was on the formation of functionalized products from biomass burning emissions, so the LC-ESI approach and results were more extensively used because they were better suited for highly-functionalized species. The compositional percentages shown in Figure 1A are shifted in an absolute sense by the exclusion of CH and CHS compounds, but particle-phase CH and CHS species were outside the scope of this study. We did not up including

the full Section S5 in the main text, but to address the reviewer's concerns we added a shorter paragraph summarizing Section S5 (lines 148-156) and included an acknowledgement in that section that LC-ESI methods excluded CH and CHS species.

*Title: It would be good to change the last word from "compounds" to "organic compounds" to make it more clear that organic compounds are the focus.*

Agreed, we have edited our title accordingly.

## **Reviewer 2**

*ACP manuscript 2020-619 reports on the detailed chemical composition of gas- and particle-phase samples collected from a boreal forest fire under ambient conditions. Samples were analyzed using gas and liquid chromatography (GC, LC) with detection by high-resolution and tandem mass spectrometry (MS, MS/MS). The focus of the analysis was on organic compounds, particularly those containing carbon, hydrogen, oxygen, nitrogen, and/or sulfate functionalities ("CHONS"); including as a function of plume age. Targeted and non-targeted approaches were used. Using both GC and LC allowed analysis of less polar (GC) and more polar/more functionalized compounds (LC) than could be achieved using a single method. Results are largely discussed in the context of elemental composition, with less focus on compound identification. It was observed that during aging particle-phase CHO compounds became less abundant, while particle-phase CHON(S) became significantly more abundant. The paper also presents precursors and pathways leading to the formation of observed sulfides included among the CHONS compounds. The paper is well written and presents interesting analysis and results that have not been presented before. The results, implications, and approach should be of interest to ACP readers. The methods are generally well described and could be reproduced based on the information provided in the SI. A few comments are provided below, both technical and editorial in content. The most significant comment on the technical side is that there are places in the manuscript where it is not clear if the compound volatility classes are being appropriately defined (i.e., based on published saturation vapor concentration ranges) based on the observed gas- and particle- phase distributions.*

We thank the reviewer for their supportive comments. We have addressed each of their comments below, including a discussion of volatility.

### **Technical Comments:**

*line 96: Is the uncertainty on the MCE values really +/- 0.4? That seems very large, given the typical range of ambient MCE values.*

We thank the reviewer for pointing this out. This was originally a typo. This has been revised in the main text to say +/- 0.01.

*Starting on line 104, the description of the volatility range of compounds sampled is a little unclear. It seems that compounds that are largely in the gas phase at OA mass loadings of 10-30 ug/m<sup>3</sup> would be classified as I/VOCs and not SVOCs. On the other end of the spectrum, C10-20*

*compounds that are largely in the gas phase may be in the VOC range (and not necessarily in the I/SVOC range).*

We thank the reviewer for pointing out this possible point of confusion for readers. We would like to clarify that all volatility bins (VOC, IVOC, SVOC, LVOC, ELVOC) were based on fixed values of saturation mass concentration,  $C^*$  (as discussed in e.g. Donahue et al., 2009, and Murphy et al., 2014) at typical OA mass loadings (e.g. 18-22  $\mu\text{g}/\text{m}^3$  of OA during the adsorbent tube sampling times). In these conditions, VOCs extend up through hydrocarbons (i.e. CH compounds) with 11 carbon atoms (specifically compounds with an n-alkane-equivalent volatility of  $C_{11}$ ). IVOCs include hydrocarbons with 12-18 carbon atoms, which are shown to equilibrate primarily to the gas-phase in outdoor conditions at the observed particle loadings. SVOCs, which begin with hydrocarbons with 19 carbon atoms, are present in both the gas- and particle-phase, with hydrocarbons less than  $C_{22}$ - $C_{23}$  existing predominantly in the gas-phase in the observed conditions. To estimate gas-particle partitioning of these  $C_{22}$ - $C_{23}$  compounds, we used the partitioning coefficient calculation described in Donahue et al., 2009 (Equation 1 in the SI), which relates the effective saturation mass concentration of mixture components to the overall OA mass loading. This is discussed in the SI (lines 230-243) and in Table S2.

To ensure that our volatility calculations and definitions were clear, we edited the Materials and Methods discussion of volatility for adsorbent tube samples (lines 113-130), and added more discussion of the volatility calculations for filter samples (lines 157-162). We also added a note at line 123 to direct readers to Section S3 and Table S2 in the SI, which discuss volatility further.

#### References:

- Donahue et al., “Atmospheric organic particulate matter: From smoke to secondary organic aerosol.” *Atmospheric Environment*, 2009
- Murphy et al., “A naming convention for atmospheric organic aerosol.” *Atmospheric Chemistry and Physics*, 2014

*This continues in 204-205, with discussion of “particle-phase” IVOCs; it isn’t clear why at mass loadings of 10-30  $\mu\text{g}/\text{m}^3$  of OA, particle-phase IVOCs would be above detection limits. By definition, such compounds are largely in the gas phase except at high OA loadings.*

The IVOCs discussed here refer specifically to functionalized particle-phase compounds, where polarity can affect partitioning behavior. We have observed particle-phase IVOCs in several past studies by our group (e.g. Ditto et al., 2018, Ditto et al., 2020) and others (e.g. studies of isoprene oxidation products that show species like 2-methyltetrols and methylglyceric acid in the particle phase, e.g. Carlton et al., *Atmos. Chem. Phys.*, 2009), which could be attributed to the presence of more polar and water-soluble compounds that are commonly observed in organic aerosol.

References:

- Ditto et al., “An omnipresent diversity and variability in the chemical composition of atmospheric functionalized organic aerosol.” *Communications Chemistry*, 2018
- Ditto et al., “Nontargeted Tandem Mass Spectrometry Analysis Reveals Diversity and Variability in Aerosol Functional Groups across Multiple Sites, Seasons, and Times of Day.” *Environmental Science and Technology Letters*, 2020
- Carlton et al., “A review of Secondary Organic Aerosol (SOA) formation from isoprene.” *Atmospheric Chemistry and Physics*, 2009

*In lines 241-243, it is suggested that compound types that have widely been observed in gas-phase smoke samples, evaporated with dilution. While a fraction of the directly emitted gas-phase compounds may partition to the particles, many of the compounds in the classes listed are not expected to contribute directly to the particle phase. Such compounds first undergo chemical transformation to create lower volatility products and then condense to the particle phase. It is not clear whether the parent compounds and their products would be observed as the same mass fragments using the techniques described.*

We thank the reviewer for pointing out this potentially confusing phrasing. In our original text, we intended to discuss the possibility of evaporation of these compound classes from particle-phase emissions, in addition to direct gas-phase emissions of these compound classes. Evaporation of particle-phase species to the gas-phase has been observed in many past studies of IVOCs and SVOCs (e.g. those referenced at line 267, in addition to other studies on the semivolatile nature of primary organic aerosol such as Robinson et al., *Science*, 2007). We have edited this section in the text to ensure that our intended meaning is clear (line 276-278).

References:

- Robinson et al., “Rethinking Organic Aerosols: Semivolatile Emissions and Photochemical Aging.” *Science*, 2007

*The discussion of volatility and partitioning needs to be carefully reviewed throughout the manuscript, and revised for accuracy, consistency, and clarity.*

We have carefully gone through the text to ensure that our discussion of volatility and partitioning was clear, and have edited language to improve clarity where needed.

*line 134: What were the “strict” QC/QA guidelines for peak retention? These are not defined in the manuscript or SI.*

A brief discussion of QA/QC was originally included in the SI in section S3.1. We added a note in the main text so readers know to consult this section for QA/QC information (line 145). We also added “QA/QC” to the section titles for S3.1 and S3.2 to emphasize this discussion. The QA/QC methods are discussed more thoroughly in the following publications referenced in the manuscript:

- Ditto et al., “An omnipresent diversity and variability in the chemical composition of atmospheric functionalized organic aerosol.” *Communications Chemistry*, 2018
- Ditto et al., “Nontargeted Tandem Mass Spectrometry Analysis Reveals Diversity and Variability in Aerosol Functional Groups across Multiple Sites, Seasons, and Times of Day.” *Environmental Science and Technology Letters*, 2020

*line 198: Is quantification of filter species affected at all by compound volatility? Or is the extraction process sufficient to extract the presumed ELVOCs with reasonable recovery?*

We expect that the filter extraction process across the reported volatility ranges should be fairly uniform. It is possible that the solvent extraction is slightly more or less effective for different chemical functionalities (i.e. compound classes), though upon testing, we did not observe any distinct trends with compound class, and the selected solvent (methanol) has been used extensively in past work (e.g. Riva et al., 2016, Surratt et al., 2008, Ng et al., 2008) that studied similarly functionalized organic aerosol species. We added a mention of this to the Supporting Information (SI line 250-252).

References:

- Riva et al., “Characterization of organosulfates in secondary organic aerosol derived from the photooxidation of long-chain alkanes.” *Atmospheric Chemistry and Physics*, 2016
- Surratt et al., “Organosulfate Formation in Biogenic Secondary Organic Aerosol.” *Journal of Physical Chemistry A*, 2008
- Ng et al., “Secondary organic aerosol (SOA) formation from reaction of isoprene with nitrate radicals (NO<sub>3</sub>).” *Atmospheric Chemistry and Physics*, 2008

*SI line 48: How was the collection efficiency of the AMS determined? Lim et al. 2019 ACP demonstrated the significant impact of CE on*

The collection efficiency of the AMS was determined using the method of Middlebrook et al. (Aerosol Science and Technology, 2012). The collection efficiency was also estimated by comparing the total mass concentrations with those derived from the UHSAS (Ultra-high sensitivity aerosol spectrometer). UHSAS volume concentrations were converted to mass concentrations using densities weighted by the AMS components. Both methods yielded similar results. In addition, there was no evidence to suggest that the AMS collection efficiency changed in and out of the fire plumes, which is consistent with previous AMS wildfire deployments (e.g. in the published data sets associated with ARCTAS – Hecobian et al., 2011; Cubison et al., 2011; SEAC4Rs – Liu et al., 2016; SCREAM – May et al., 2015). We have added a mention of these methods to the Supporting Information (SI line 47-52).

References:

- Middlebrook et al., "Evaluation of Composition-Dependent Collection Efficiencies for the Aerodyne Aerosol Mass Spectrometer using Field Data." *Aerosol Science and Technology*, 2012
- Hecobian et al., "Comparison of chemical characteristics of 495 biomass burning plumes intercepted by the NASA DC-8 aircraft during the ARCTAS/CARB-2008 field campaign." *Atmospheric Chemistry and Physics*, 2011
- Cubision et al., "Effects of aging on organic aerosol from open biomass burning smoke in aircraft and laboratory studies." *Atmospheric Chemistry and Physics*, 2011
- Liu et al., "Agricultural fires in the southeastern U.S. during SEAC<sup>4</sup>RS: Emissions of trace gases and particles and evolution of ozone, reactive nitrogen, and organic aerosol." *Journal of Geophysical Research: Atmospheres*, 2016
- May et al., "Observations and analysis of organic aerosol evolution in some prescribed fire smoke plumes." *Atmospheric Chemistry and Physics*, 2015

*SI line 83: I'm assuming that the field blanks were used to correct for background, and not to reduce background as stated here.*

Yes, blanks were used to account and correct for any contamination in the sampling and analytical systems. We have changed the word "reduce" to "correct for", now at SI line 87.

*Editorial Comments: line 62: In this context, what is meant by "unprecedented"? Is it in reference to the analytical techniques used? Or the extent of chemical composition data obtained? Other?*

In this context, we used "unprecedented" to mean that the analytical methods and degree of chemical speciation were novel. We removed the term to reduce possible confusion.

*line 113: No hyphen is needed between "gas" and "phase" (also in line 224 in the SI).*

These have been corrected.

*SI line 75: remove one of the "s" on "VOCs"*

Corrected.

*line 129: "mode" should be plural*

Corrected.

*SI line 295: suggest to move the Kroll et al reference as it suggests the values themselves (rather than the approach) are from Kroll et al.*

We moved the reference so that it appears earlier in the sentence.

1 **Atmospheric Evolution of Emissions from a Boreal Forest Fire: The Formation of Highly-**  
2 **Functionalized Oxygen-, Nitrogen-, and Sulfur-Containing Organic Compounds**

3  
4 Jenna C. Ditto<sup>1</sup>, Megan He<sup>1</sup>, Tori N. Hass-Mitchell<sup>1</sup>, Samar G. Moussa<sup>2</sup>, Katherine Hayden<sup>2</sup>,  
5 Shao-Meng Li<sup>2</sup>, John Liggio<sup>2</sup>, Amy Leithead<sup>2</sup>, Patrick Lee<sup>2</sup>, Michael J. Wheeler<sup>2</sup>,  
6 Jeremy J.B. Wentzell<sup>2</sup>, Drew R. Gentner<sup>1,3,\*</sup>

7  
8 <sup>1</sup> Department of Chemical and Environmental Engineering, Yale University, New Haven, CT,  
9 06511, USA; <sup>2</sup> Air Quality Research Division, Environment and Climate Change Canada,  
10 Toronto, Ontario M3H 5T4, Canada; <sup>3</sup> Solutions for Energy, Air, Climate and Health  
11 (SEARCH), School of the Environment, Yale University, New Haven CT 0651, USA

12  
13 \* Correspondence to: [drew.gentner@yale.edu](mailto:drew.gentner@yale.edu)

14  
15 **Abstract**

16 Forest fires are major contributors of reactive gas- and particle-phase organic compounds  
17 to the atmosphere. We used offline high resolution tandem mass spectrometry to perform a  
18 molecular-level speciation of gas- and particle-phase compounds sampled via aircraft from an  
19 evolving boreal forest fire smoke plume in Saskatchewan, Canada. We observed diverse  
20 multifunctional compounds containing oxygen, nitrogen, and sulfur (CHONS), whose structures,  
21 formation, and impacts are understudied. The dilution-corrected absolute ion abundance of  
22 particle-phase CHONS compounds increased with plume age by a factor of 6.4 over the first 4  
23 hours of downwind transport, and their relative contribution to the observed functionalized

24 organic aerosol (OA) mixture increased from 19% to 40%. The dilution-corrected absolute ion  
25 abundance of particle-phase compounds with sulfide functional groups increased by a factor of  
26 13 with plume age, and their relative contribution to observed OA increased from 4% to 40%.  
27 Sulfides were present in up to 75% of CHONS compounds and the increases in sulfides were  
28 accompanied by increases in ring-bound nitrogen; both increased together with CHONS  
29 prevalence. A complex mixture of intermediate- and semi-volatile gas-phase organic sulfur  
30 species was observed in emissions from the fire and depleted downwind, representing potential  
31 precursors to particle-phase CHONS compounds. These results demonstrate CHONS formation  
32 from nitrogen/oxygen-containing biomass burning emissions in the presence of reduced sulfur  
33 species. In addition, they highlight chemical pathways that may also be relevant in situations  
34 with elevated emissions of nitrogen- and sulfur-containing organic compounds from residential  
35 biomass burning and fossil fuel use (e.g. coal), respectively.

36

## 37 **1 Introduction**

38 Forest fires are predicted to become increasingly prevalent and severe with climate  
39 change (Abatzoglou and Williams, 2016; Barbero et al., 2015; Jolly et al., 2015). These fires are  
40 an important and uncontrolled source of gas- and particle-phase compounds to the atmosphere,  
41 including a complex mixture of gas-phase reactive organic carbon, primary organic aerosol  
42 (POA), carbon monoxide, carbon dioxide, methane, ammonia, nitrogen oxides, and black carbon  
43 (Akagi et al., 2011; Gilman et al., 2015; Hatch et al., 2015, 2018; Koss et al., 2018; Vicente et  
44 al., 2013; Yokelson et al., 2013). Many of these emitted compounds are precursors to downwind  
45 ozone and secondary organic aerosol (SOA) production (Ahern et al., 2019; Buysse et al., 2019;  
46 Gilman et al., 2015; Hennigan et al., 2011; Lim et al., 2019).

47 Primary and secondary pollutants from biomass burning have important effects on air  
48 quality locally, regionally, and continentally (Burgos et al., 2018; Colarco et al., 2004; Cottle et  
49 al., 2014; Dreessen et al., 2016; Forster et al., 2001; Rogers et al., 2020; Val Martín et al., 2006),  
50 and their impacts on human health and climate (e.g. via light absorbing brown and black carbon)  
51 have been well documented (Forrister et al., 2015; Jiang et al., 2019; Liu et al., 2017; Di Lorenzo  
52 et al., 2018; Reid et al., 2016; Sengupta et al., 2018; Wong et al., 2019). These health and climate  
53 effects are sensitive to the elemental and structural composition of gas- and particle-phase  
54 emissions and transformation products (Hallquist et al., 2009; Nozière et al., 2015). As a result,  
55 past studies have used online and offline mass spectrometry techniques to characterize the  
56 chemical composition of fresh and aged biomass burning [emissions](#) and have revealed a wide  
57 array of emitted hydrocarbons and oxygen-, nitrogen-, or sulfur-containing functionalized  
58 species (Ahern et al., 2019; Bertrand et al., 2018; Gilman et al., 2015; Hatch et al., 2015, 2018,  
59 2019; Inuma et al., 2010; Koss et al., 2018; Laskin et al., 2009; Yokelson et al., 2013).  
60 However, the emissions and chemical transformations occurring in ambient biomass burning  
61 plumes are extremely complex and despite previous measurements remain poorly understood at  
62 the molecular-level.

63 In this study, we used an aircraft sampling system developed to collect offline gas- and  
64 particle-phase organic compounds [above](#) a boreal forest fire. We examined the molecular-level  
65 emissions and evolution of the forest fire plume [via an](#) analysis of [these](#) offline samples using  
66 gas and liquid chromatography (GC/LC) with high resolution mass spectrometry (MS), including  
67 tandem mass spectrometry (MS/MS). This degree of detailed chemical speciation is important to  
68 advance knowledge of in-plume chemical pathways and reaction products, long-distance

69 transport, and fate of biomass burning products—all of which will improve modeling capabilities  
70 and our understanding of the health and environmental impacts of biomass burning.

71 Specifically, the goals of this study were: (1) to perform a detailed speciation of gas- and  
72 particle-phase organic compounds derived from the boreal forest fire in terms of elemental and  
73 functional group composition, to assess changes in composition at the molecular-level as the  
74 plume aged; and (2) to examine the evolution of oxygen-, nitrogen-, and sulfur-containing  
75 (CHONS) compounds. These CHONS compounds made up 19-40% of functionalized [OA](#) here  
76 and have been observed at other ambient sites (e.g. 9-11% (Ditto et al., 2018)), though little is  
77 known about their structures or formation mechanisms. Using our observations of gas-phase  
78 sulfur species, we identified possible precursors and reaction pathways involved in the formation  
79 of these CHONS compounds.

80

## 81 **2 Materials and Methods**

82 On June 25th, 2018, two research flights were conducted by Environment and  
83 Climate Change Canada as part of their Air Pollution research program. These flights sampled  
84 two boreal wildfire smoke plumes originating near Lac La Loche in northern Saskatchewan,  
85 Canada (Figure S1). The region is dominated by pine and spruce trees (Canada's National Forest  
86 Inventory, 2020). Gas- and particle-phase samples were collected from the National Research  
87 Council of Canada's Convair-580 research aircraft for analysis with offline high resolution mass  
88 spectrometry, alongside many other measurements (Supporting Information S1-S2). The aircraft  
89 flew the same straight-line tracks at multiple altitudes through the smoke plumes ([average](#)  
90 [altitudes shown in Table S1](#)), which when stacked created a virtual screen intercepting the  
91 plumes at each of five downwind locations ([with](#) flight design similar to those previously

92 reported (Li et al., 2017; Liggio et al., 2016)). Screen 1 was ~10 km from the fire with screens 2-  
93 4 following the plumes downwind, and screen 5 intercepting the plumes after they had passed  
94 over several major surface and in-situ mining oil sands facilities (Figure S1). The samples  
95 discussed here were collected across both plumes to ensure that enough mass was present to [well](#)  
96 surpass the mass spectrometer's detection limits. Based on satellite information and aircraft  
97 measurements at the start of sampling (i.e. screen 1), the fire was a low-intensity surface fire  
98 with smoldering conditions; aircraft measurements indicated a modified combustion efficiency  
99 of  $0.90 \pm 0.01$  for both plumes.

100 Combined gas- and particle-phase samples were collected onto custom adsorbent tubes  
101 packed with high-purity quartz wool, glass beads, Tenax TA, and Carbopack X (Sheu et al.,  
102 2018). Samples were collected along screens 1-4 in Figure S1 (no adsorbent tubes collected at  
103 screen 5) via an external pod mounted under the wing of the aircraft, which included remote  
104 switching between adsorbent tubes at various transect altitudes and online measurements of  
105 temperature, pressure, and flow (Supporting Information S1, Figure S2).

106 All adsorbent tubes were analyzed using a GERSTEL Thermal Desorber TD 3.5+ with  
107 gas chromatography (Agilent 7890B GC), atmospheric pressure chemical ionization (APCI), and  
108 quadrupole time-of-flight mass spectrometry (Agilent 6550 Q-TOF), similar to past work (Khare  
109 et al., 2019). For adsorbent tubes, the APCI was operated in positive ionization mode and the Q-  
110 TOF was operated in MS mode (i.e. TOF data collection only, hereafter “GC-APCI-MS”).

111 Adsorbent tube data were processed primarily via a targeted approach for  $C_xH_y$ ,  $C_xH_yO_l$ ,  $C_xH_yS_l$ ,  
112 and  $C_xH_yN_l$  compounds using custom Igor Pro code (Supporting Information S2-S3).

113 In order to reduce losses of lower volatility gases onto upstream surfaces, particles were  
114 not explicitly filtered out at the inlet of the wing-pod sampler used for adsorbent tube collection.

115 For several reasons, it was concluded that the  $C_xH_y$  hydrocarbons smaller than  $C_{22-23}$  (and  
116  $C_xH_yS_1/C_xH_yO_1/C_xH_yN_1$  compounds of similar volatility) measured in the adsorbent tubes were  
117 predominantly in the gas-phase. This was based on (1) significant undersampling for particles at  
118 the wing pod inlet since the adsorbent tube sampling flow rate was a factor of  $\sim 4$  lower than its  
119 corresponding isokinetic flow rate, resulting in a significant divergence of particles away from  
120 the inlet during sampling; and (2) partitioning theory, using average in-plume organic aerosol  
121 (OA) concentrations of  $18-22 \mu\text{g}/\text{m}^3$  across adsorbent tube sampling periods for screens 1-4,  
122 concurrently measured by an aerosol mass spectrometer (AMS) onboard the aircraft (see  
123 Supporting Information S1, S3, Table S2). Thus, the  $C_{22}$  and smaller  $C_xH_y$  compounds (and other  
124 compound classes of similar volatility) should have primarily been in the gas phase at  
125 equilibrium. As such, we limited the following adsorbent tube data analysis to compounds in the  
126  $C_{10}-C_{25}$  range to focus on intermediate-volatility and semivolatile (I/SVOCs) compounds present  
127 in the gas phase. In our analyses and interpretation, the compounds included in each of these  
128 volatility ranges are defined based on fixed values of saturation mass concentrations (e.g.  
129 Donahue et al., 2011; Murphy et al., 2014) at the observed  $18-22 \mu\text{g}/\text{m}^3$  OA loadings present  
130 during adsorbent tube sampling times.

131         Dedicated particle-phase samples were collected on 47 mm PTFE filters (2.0  $\mu\text{m}$  pore;  
132 Pall Corporation) from a sampling manifold in the aircraft cabin containing six independent  
133 anodized aluminum filter holders. The filters were sampled behind an isokinetic inlet with a size  
134 cutoff of approximately 2.5  $\mu\text{m}$ . One filter sample was collected per screen for screens 1-5  
135 shown in Figure S1.

136         Filter samples were extracted in methanol (Ditto et al., 2018). Samples were analyzed via  
137 liquid chromatography (Agilent 1260 LC) with electrospray ionization (ESI) and the same Q-

138 TOF. For filters, the ESI source was operated in both positive and negative ionization modes,  
139 and the Q-TOF was operated in both MS mode (i.e. TOF data collection, “LC-ESI-MS”) and  
140 MS/MS mode (i.e. tandem mass spectral data collection, “LC-ESI-MS/MS”) (Ditto et al., 2018,  
141 2020). Filter extracts were also analyzed using GC-APCI-MS in positive ionization mode. Filter  
142 data from LC-ESI-MS, LC-ESI-MS/MS, and GC-APCI-MS were analyzed with a non-targeted  
143 approach, using Agilent Mass Hunter, SIRIUS with CSI:FingerID, and custom R code  
144 (Supporting Information S2-S3) (Ditto et al., 2018, 2020). All peaks that passed strict [QA/QC](#)  
145 [\(Section S3\)](#) were assigned molecular formulas, with candidate formulas limited to 20 oxygen, 3  
146 nitrogen, and/or 1 sulfur atom(s). [Hereafter, LC-ESI](#) compound classes are discussed here  
147 without subscripts.

148 [The particle-phase compounds observed via LC-ESI vs. GC-APCI techniques varied](#)  
149 [significantly in their oxygen, nitrogen, and sulfur content since these two chromatographic and](#)  
150 [ionization approaches are sensitive towards different types of compounds \(see Section S5\). As](#)  
151 [the forest fire plume aged, the complex mixture of emissions and secondary products became](#)  
152 [increasingly functionalized and thus less GC-amenable without derivatization. Therefore, we](#)  
153 [focused on LC-ESI-MS data to study these functionalized particle-phase compounds. We](#)  
154 [acknowledge that this method excludes fully-reduced hydrocarbons and fully-reduced sulfur-](#)  
155 [containing particle-phase compounds \(i.e. CH and CHS \(Ditto et al., 2018\)\) and thus these](#)  
156 [compound classes are not accounted for in the relative particle-phase distributions shown here.](#)

157 [For particle-phase analyses, we estimated saturation mass concentration based on the Li](#)  
158 [et al. parameterization \(Li et al., 2016\), then grouped compounds based on fixed volatility bins](#)  
159 [\(Donahue et al., 2011; Murphy et al., 2014\). Particle-phase compounds were observed across the](#)  
160 [IVOC, SVOC, LVOC, and ELVOC ranges. Particle-phase IVOCs have been observed in the](#)

161 past, and despite their higher volatility, may exist in the particle-phase due to their polarity and  
162 water solubility. Additional details on these methods, including a discussion of total mass  
163 analyzed from filters/adsorbent tubes and QA/QC, are discussed in Supporting Information S1-  
164 S5, with a methods summary shown in Figure S3.

### 166 3 Results

#### 167 3.1 Evolution of organic aerosol elemental composition and functionality with plume age

168 Our analysis of functionalized OA showed several compositional trends in the evolving  
169 boreal forest fire smoke plume (screens 1-4) and exhibited marked changes after emissions from  
170 the oil sands facilities were mixed with the forest fire plume (screen 5). Here, we focused on the  
171 forest fire plume in screens 1-4. We observed a diverse elemental composition in functionalized  
172 OA across oxygen-, nitrogen-, and/or sulfur-containing compound classes (Figure 1A-1B, Figure  
173 S5). This included oxygenates (CHO), such as common biomass burning tracers and their  
174 isomers (e.g. levoglucosan, Supporting Information S2); as well as oxygen- and nitrogen-  
175 containing compounds (CHON); oxygen- and sulfur-containing compounds (CHOS); reduced  
176 nitrogen-containing compounds (CHN); reduced nitrogen- and sulfur-containing compounds  
177 (CHNS); as well as compounds containing oxygen, nitrogen, and sulfur (CHONS).

178 There was a continual decrease in the relative abundance of particle-phase CHO  
179 compounds in the observed functionalized OA across screens 1-4, accompanied by a consistent  
180 relative increase in CHON and CHONS compounds (Figure 1B). Notably, the relative abundance  
181 of CHONS compounds increased from 19% to 40% of measured functionalized OA from screens  
182 1 to 4. Trends in absolute ion abundances were also similar (note: carbon monoxide mixing ratio  
183 was used to account for dilution). This is shown in Figure 1C (inset) and Figure S5C; CHO

184 generally decreased from screens 1 to 4, while CHONS and CHON generally increased,  
185 suggesting that CHONS compounds were possibly formed from CHO, CHN, and/or CHON  
186 precursors in the gas- and/or particle-phases. Specifically, the dilution-corrected abundance of  
187 CHONS species increased by a factor of 6.4 from screen 1 to 4 (Figure 1C, inset). In Figure 1,  
188 we primarily presented data as relative contributions to functionalized OA to examine changes in  
189 the evolution of the complex mixture as a whole and the relationships between different  
190 compound classes and functional groups with plume age. However, dilution-corrected  
191 abundances are also important for understanding absolute formation (or depletion), and are  
192 shown for all species in Figures S5-S6.

193 Based on MS/MS analyses, these evolving CHO, CHN, CHON, and CHONS compounds  
194 were often comprised of variable combinations of hydroxyl and ether functional groups (e.g.  
195 primary emissions from forest fires like methoxyphenols and similar structures), as well as  
196 amine, imine, and sulfide groups, along with cyclic nitrogen structural features (consistent with  
197 past laboratory observations of biomass burning emissions (Laskin et al., 2009; Lin et al., 2018;  
198 Liu et al., 2015; Updyke et al., 2012)).

199

### 200 3.2 Detailed speciation of CHONS compounds in functionalized OA

201 While some individual CHONS species contained grouped oxygen, nitrogen, and sulfur  
202 atom moieties (e.g. sulfonamides), the majority of CHONS compounds had a combination of  
203 multiple separate oxygen-, nitrogen-, and/or sulfur-containing functional groups (Figure 2A-2B).  
204 Sulfide groups were important contributors to CHONS compounds (Figure 2B) and showed a  
205 notable increase in relative contribution to the overall functional group distribution with plume  
206 age (Figure 1C). They increased from 4% to 40% of measured compound abundance across

207 screens 1 [to](#) 4 (Figure 1C), [which corresponded to an increase by a factor of 13 in terms of their](#)  
208 [dilution-corrected abundance \(Figure 1C, inset\)](#). Their increasing relative contribution to  
209 CHONS compounds with plume evolution was even more pronounced—by screen 4, the sulfide  
210 functional group was present in 75% of detected CHONS compound abundance (Figure S7A).  
211 Here, we focused on the presence of sulfides in CHONS compounds because most of the  
212 observed particle-phase sulfides occurred as part of CHONS species (71%), while a smaller  
213 fraction occurred [in](#) CHOS (21%) or CHNS (8%) [compounds](#) (Figure 3A).

214 To explore possible precursors and formation pathways for these particle-phase sulfide-  
215 containing CHONS species, we used MS/MS to identify nitrogen-containing functional groups  
216 that co-occurred with sulfides. In CHONS compounds, most sulfides co-occurred with cyclic  
217 nitrogen (36% [of sulfide-containing species](#)), amine (32%), or imine features (43%) (Figure 3B).  
218 The prevalence of sulfide and cyclic nitrogen features in the measured functionalized OA  
219 increased together screen-to-screen, and increased together with the rising proportion of CHONS  
220 compounds (Figure 3C). While sulfides often co-occurred with amines or imines and while  
221 amines and imines were prevalent in all 4 screens (Figure 1C), there was no relationship between  
222 [these functional groups](#) and the increasing contribution of CHONS compounds to measured  
223 functionalized OA (Figure S7B).

224 The sulfide substructures observed via MS/MS often contained linear carbon chains or  
225 phenyl groups bonded to the sulfur atom (Figure 3C inset). Thus, we hypothesize that precursors  
226 with similar reduced sulfur-containing structures reacted with cyclic nitrogen-containing species  
227 to form the observed [particle-phase](#) sulfide-containing CHONS compounds [\(see further](#)  
228 [discussion of possible](#) precursors in Section 3.3, [and](#) potential chemical pathways in Section [4.2](#)).

229 CHONS compounds were predominantly SVOCs in screens 1-4 (i.e. 89% of CHONS ion  
230 abundance, Figure 2C, Figure S8), suggesting that these compounds were formed from higher  
231 volatility gas-phase species. In contrast, with the added influence of the oil sands facilities in  
232 screen 5, 68% of CHONS compounds were extremely low volatility organic compounds  
233 (ELVOCs), though CHONS made up only 2% of functionalized OA at screen 5.

234 Overall, dilution-corrected abundances of functionalized OA in each particle-phase  
235 volatility bin increased with plume age, but the relative contribution of SVOCs increased from  
236 37% to 58% while the relative contribution of IVOCs dropped from 38% to 20%, potentially due  
237 to oxidation reactions that formed SVOCs and/or due to evaporation (Figure S9). These particle-  
238 phase IVOCs consisted predominantly of CHO, CHN, and CHON ( $O/N < 3$ ) compounds, which  
239 could include possible non-sulfur containing precursors to the observed CHONS species.  
240 Fragmentation of particle-phase L/ELVOC compounds also could have contributed to some of  
241 the observed SVOC mass, but the overall increasing total abundance across all volatility bins  
242 with plume age supports the idea that these compounds were predominantly formed from more  
243 volatile precursors (e.g. I/SVOCs).

244

### 245 3.3 Targeted search for CHONS precursors in the gas-phase

246 To investigate the precursors and chemistry that could have formed the sulfide-containing  
247 CHONS species observed in the particle-phase samples, we performed a targeted search for  
248 possible gas-phase I/SVOC species in each adsorbent tube, across all  $C_{10}$ - $C_{25}$   $C_xH_yS_1$  species  
249 with the equivalent of 0-15 double bonds and/or rings (i.e.  $C_xH_{2x+2}S_1$ -  $C_xH_{2x-28}S_1$ , Figure 4A,  
250 Figure S10). We observed a distribution of  $C_xH_yS_1$  compounds and their isomers; based on the  
251 high mass resolution and high mass accuracy molecular formulas from targeted GC-APCI-MS

252 analysis, 27% of  $C_xH_yS_1$  compounds were fully saturated (i.e.  $C_xH_{2x+2}S_1$ ) and 25% contained the  
253 equivalent of 4-6 double bonds and/or rings (i.e.  $C_xH_{2x-6}S_1$ -  $C_xH_{2x-10}S_1$ ), which included single  
254 ring aromatics. We focused on these sulfur-containing gases as candidate precursors to the  
255 observed particle-phase sulfide-containing CHONS compounds as they contained sulfur  
256 substructures with linear carbon chains or phenyl groups, similar to those observed on particle-  
257 phase CHONS compounds via MS/MS analysis (Figure 3C inset, Figures S10-S11). However,  
258 we also observed contributions from other sulfur-containing structures (e.g. with the equivalent  
259 of 1-3 double bonds and/or rings, Figure 4A), which could also have been precursor species.

260 The observed gas-phase  $C_{10}$ - $C_{25}$   $C_xH_yS_1$  compounds were present in gas-phase emissions  
261 from the fire and likely also evaporated from primary OA during early plume dilution. Gas-phase  
262  $C_{10}$ - $C_{25}$   $C_xH_yS_1$  concentrations increased relative to carbon monoxide from screen 1 to 2, then  
263 steadily decreased with plume age (Figure 4B, Figure S12A). This suggests the gas-phase  
264 emission and/or evaporation of  $C_xH_yS_1$  compounds from OA between screens 1 and 2, and  
265 subsequent participation in plume chemistry from screens 2 to 4.

266 Similar OA evaporation with plume dilution has been observed in many past studies  
267 (Ahern et al., 2019; Garofalo et al., 2019; Hennigan et al., 2011; Lim et al., 2019). To better  
268 understand the dynamics of these sulfur-containing compounds and their possible particle-phase  
269 origin, we compared their concentrations to those of  $C_{10}$ - $C_{25}$  aliphatic and aromatic  $C_xH_y$  and  
270  $C_xH_yO_1$  species from a similar targeted search of adsorbent tube gas-phase compounds. Overall,  
271  $C_xH_y$  and  $C_xH_yO_1$  compound classes dominated the observed  $C_{10}$ - $C_{25}$  compounds (Figure 4B,  
272 Figure S12B), with 61%  $C_xH_y$ , 36%  $C_xH_yO_1$ , and just 3%  $C_xH_yS_1$  on average.  $C_xH_y$  and  $C_xH_yO_1$   
273 concentrations generally increased with plume age (Figure 4B) and included many known  
274 compound types (e.g. monoterpenes, aromatics, hydroxyls, carbonyls (Akagi et al., 2011;

275 Andreae, 2019; Gilman et al., 2015; Hatch et al., 2015, 2019; Koss et al., 2018)). This suggests  
276 the direct emission of these gas-phase compound classes from the fire (observed at screen 1)  
277 along with the evaporation of semivolatile particle-phase emissions as the plume evolved, and  
278 formation of  $C_xH_yO_1$  via  $C_xH_y$  oxidation. AMS measurements of total OA concentrations  
279 provided supporting evidence of OA evaporation; the ratio of AMS OA concentration to CO  
280 decreased by 7% from screen 1 to 2 (corresponding to an AMS OA/CO ratio of -0.0044 or a  
281 decrease in OA concentrations of  $-2.3 \mu\text{g}/\text{m}^3$ ), while the ratio of total gas-phase  $C_xH_y$ ,  $C_xH_yO_1$ ,  
282 and  $C_xH_yS_1$  concentration to CO increased by 55% (corresponding to a total gas-phase  
283 concentration/CO ratio of 0.022 or an increase in gas-phase concentration of  $7.0 \mu\text{g}/\text{m}^3$ , with  
284 changes summarized in Table S3). While not the focus of the analytical approaches applied in  
285 this study, to further substantiate the observation of OA evaporation, we performed the same  
286 targeted analysis of  $C_{10}$ - $C_{25}$   $C_xH_y$ ,  $C_xH_yO_1$ , and  $C_xH_yS_1$  compounds in the particle-phase filter  
287 sample extracts analyzed via GC-APCI-MS. We observed a similar decrease in concentration  
288 from screen 1 to 2. However, these filter measurements (even with APCI ionization) were not  
289 geared towards  $C_xH_y$  and  $C_xH_yS_1$  speciation due to possible solubility limitations in the  
290 extraction solvent (Supporting Information S4). Direct thermal desorption of quartz filters with  
291 GC-APCI analysis would be better suited for these  $C_xH_y$  and  $C_xH_yS_1$  measurements (as  
292 performed in this study with adsorbent tubes).

293 As discussed in *Materials and Methods*, the observed compounds with volatilities below  
294 that of  $\sim C_{22}$ - $C_{23}$  hydrocarbons existed primarily in the gas-phase (Table S2), while larger  
295 compounds favored the particle-phase (with a smaller fraction in the gas-phase at equilibrium).  
296 The presence of gas-phase compounds across this I/SVOC range (e.g. Figures S10, S13) further  
297 corroborates the possibility of contributions from both direct gas-phase emissions and from

298 evaporation [of particle-phase emissions](#) (Supporting Information S3). In contrast to  $C_xH_y$   
299 concentrations,  $C_xH_yS_1$  concentrations dropped markedly after screen 2 despite similarities in the  
300 volatility distribution of  $C_xH_y$  and  $C_xH_yS_1$  I/SVOC mixtures (Figure 4A, Figures S10 and S13).  
301 This difference [across screens](#) shows that the observed  $C_xH_yS_1$  I/SVOCs were removed ([e.g. via](#)  
302 [chemical reactions](#)) more [quickly](#) than  $C_xH_y$  ([Figure 4B](#)), thus supporting their potential  
303 contribution to CHONS formation.

304 In addition to the  $C_{10}$ - $C_{25}$   $C_xH_yS_1$  compounds measured in the adsorbent tubes, smaller  
305 sulfur-containing compounds could have also acted as CHONS precursors, like those identified  
306 by the onboard proton transfer reaction-mass spectrometer (PTR-ToF-MS). While dimethyl  
307 sulfide (DMS, previously observed in biomass burning smoke (Andreae, 2019)) was often below  
308 [the instrument's](#) limit of detection, both dimethyl and diethyl sulfide showed good correlation  
309 with acetonitrile ([a well-known biomass burning product \(Andreae, 2019\)](#)) in the smoke plume  
310 during screen 1 ( $r \sim 0.95$ , Figure S12C). This suggests that these compounds were co-emitted by  
311 the fire.

312

## 313 **4 Discussion**

### 314 4.1 Investigating possible origins of gas-phase sulfur compounds

315 The gas-phase sulfur-containing compounds observed in the plume were emitted from the  
316 smoldering fire. However, their origins are uncertain, since the broader range of sulfur species  
317 found here (Figure 4A, Figures S10-11) has not been [previously](#) reported; many of the  
318 compounds in the complex [mixture of sulfur-containing compounds discussed in this work](#) were  
319 outside the detection range [of](#) previously employed methods (Hatch et al., 2015; Khare et al.,  
320 2019; Koss et al., 2018; Sekimoto et al., 2018). Here, we explore two potential origins of these

321 gas-phase sulfur-containing precursors to the observed particle-phase CHONS compounds: the  
322 biomass fuel itself and the deposition of sulfur species from anthropogenic/industrial operations.

323 *Fuel:* In past studies, emissions of sulfur-containing organic compounds were typically  
324 minor compared to oxygen- or nitrogen-containing compounds, and the relative balance of  
325 oxygen-, nitrogen-, or sulfur-containing compound emissions was typically proportional to fuel  
326 content (Hatch et al., 2015; Ward, 1990). The estimated N:S ratio for boreal forest fuel near the  
327 fire was ~10:1 (Huang and Schoenau, 1996), which was similar to the average N:S ratio from a  
328 non-targeted search for nitrogen- and sulfur-containing I/SVOCs from the adsorbent tube  
329 samples in this study of  $(8.1 \pm 4.8):1$ . Sulfur is an essential nutrient in plants, and can be taken up  
330 from soil (as sulfate) or from the atmosphere via deposition (as SO<sub>2</sub> and sulfate) (Aas et al.,  
331 2019; Gahan and Schmalenberger, 2014; Leustek, 2002). Both SO<sub>2</sub> and sulfate are metabolized  
332 in plants to yield a variety of compounds critical to plant functions including cysteine and a  
333 range of other sulfur- (as well as oxygen- and nitrogen-) containing compounds (Leustek, 2002).  
334 In addition, disulfide bonds contribute to plant protein structure, and these bonds can cleave and  
335 form thiols (Gahan and Schmalenberger, 2014; Leustek, 2002; Onda, 2013). Sulfur-containing  
336 compounds like these may have been emitted during the fire, along with other known sulfur  
337 products from boreal fuels (e.g. DMS, thiophenes (Akagi et al., 2011; Hatch et al., 2015; Koss et  
338 al., 2018; Landis et al., 2018)).

339 *Deposition:* While sulfur can be naturally occurring, it is also associated with  
340 anthropogenic activities (e.g. transportation, power generation, industry, etc.). A portion of the  
341 sulfur in the forest fire emissions could have originated from sulfur deposited via such  
342 anthropogenic activities. The closest large anthropogenic sulfur source to the fire location was  
343 the oil sands mining region north of Fort McMurray, Alberta, which was approximately 150 km

344 away and which contains known SO<sub>2</sub> emitters (Liggio et al., 2017; McLinden et al., 2016).  
345 Regional concentrations of SO<sub>2</sub> or other sulfur species from these nearby industrial activities  
346 could have led to accumulated deposition of inorganic and/or organic sulfur compounds over  
347 time, though it is uncertain how much of this deposited sulfur would have been taken up and  
348 transformed by vegetation due to sulfur uptake and assimilation regulatory pathways in plants  
349 (Davidian and Kopriva, 2010). This possible accumulated deposition may have acted as a  
350 reservoir of sulfur to be emitted during fires via the re-volatilization of deposited compounds, in  
351 addition to the evaporation of typical sulfur metabolites or the formation of sulfur-containing  
352 combustion by-products. This hypothesis is consistent with recent deposition measurement and  
353 modeling results for the region, which indicated that sulfur deposition from the oil sands  
354 [operations](#) potentially impacted areas downwind, including the region where this fire occurred  
355 (Makar et al., 2018).

356 Interestingly, lichen and spruce trees, which are prominent in the region of the fire  
357 discussed here, have been reported to accumulate sulfur from SO<sub>2</sub> in regions near large industrial  
358 SO<sub>2</sub> sources (Meng et al., 1995; Nyborg et al., 1991). Also, past studies have reported  
359 enhancements in sulfate (as well as nitrate/ammonium) aerosols [coming](#) from biomass burning in  
360 areas with urban influence (Fenn et al., 2015; Hecobian et al., 2011; Hegg et al., 1987).  
361 Inorganic aerosol components from both urban (e.g. Edmonton, Alberta) and industrial (e.g. oil  
362 sands) sources could deposit in the area surrounding the emissions source along with an organic  
363 phase, which we postulate could contain a range of sulfur-containing species including the  
364 C<sub>x</sub>H<sub>y</sub>S<sub>1</sub> compounds shown here. [These deposited inorganic and organic species may have re-](#)  
365 [volatilized during the fire](#). However, further work is needed to disentangle the contribution of  
366 natural vs. anthropogenic sulfur to biomass burning [emissions in the region](#). [Also, we note that](#)

367 the fire was ~1 hour old at the time of sampling, so the recent application of fire suppressants  
368 was unlikely to contribute to the species observed.

#### 370 4.2 Potential reaction pathways leading to sulfides in CHONS from sulfur precursors

371 A number of potential reactions involving sulfur-containing precursors, often thiols (R-  
372 SH), may have contributed to the formation of the observed sulfide functional groups in particle-  
373 phase CHONS compounds (Figure S14). On average, our gas-phase measurements were  
374 comprised of 27% fully saturated sulfur-containing hydrocarbons (i.e.  $C_xH_{2x+2}S_1$ , Figures S10-  
375 11). It is likely that some fraction of the sulfur compounds observed in the gas-phase adsorbent  
376 tube measurements (e.g. the compounds identified as  $C_xH_{2x+2}S_1$ ) and in PTR-ToF-MS  
377 measurements (e.g. dimethyl sulfide, diethyl sulfide) were thiols, but the distinction between  
378 sulfide vs. thiol isomers was challenging with these methods without specific internal standards.

379 In some of the following possible reactions, a thiol interacts with a non-sulfur precursor  
380 to yield a sulfide-containing compound. The non-sulfur precursor (in the gas- or particle-phase)  
381 may have contained O and N atoms, thus yielding a CHONS compound immediately after  
382 participating in one of the proposed reactions. Alternatively, the newly formed sulfide-containing  
383 compound may have undergone subsequent, separate reactions with oxygen- and/or nitrogen-  
384 containing species (in the gas- or particle-phase) to form the observed sulfide-containing  
385 CHONS species. Here, we focused on possible reactions that could have contributed the sulfide  
386 group to these oxygen- and/or nitrogen-containing compounds (known emissions from forest  
387 fires, as discussed above). Earlier, we postulated that because most of the observed particle-  
388 phase CHONS compounds were SVOCs, these compounds were predominantly formed by  
389 reactions with more volatile gas-phase compounds. However, it is uncertain whether these

390 sulfide-forming and CHONS-forming reactions [all](#) occurred in the gas-phase with subsequent  
391 partitioning to the particle-phase, heterogeneously, or in a combination of separate gas- and  
392 particle-phase chemistry. We suggest some possible sulfide-forming reactions here, yet we note  
393 that these proposed reactions are likely not comprehensive. Further work to elucidate the  
394 chemistry driving this sulfide and CHONS formation is needed.

395         Some possible reactions include: (1) thiol-ene reactions, where a thiol reacts with an  
396 alkene (or alkyne), which can form carbon-sulfur bonds (Lowe, 2010). Alkenes are known to be  
397 prominent in emissions from boreal fires (Gilman et al., 2015; Hatch et al., 2015), and we  
398 observed similar structures in our gas-phase samples that likely included alkenes, cyclic alkanes,  
399 and/or monoterpenes (Figure S13). (2) Thiol reactions with carbonyls, which can form  
400 hemithioacetals that subsequently dehydrate in the atmosphere to yield sulfides (Jencks and  
401 Lienhard, 1966). This reaction is similar to the formation of enamines from carbonyls and  
402 dimethyl amine via the formation and subsequent dehydration of a carbinolamine, which has  
403 been shown to occur in ambient conditions (Duporté et al., 2016, 2017). (3) Thiol reactions with  
404 alcohols, which can form sulfides; [these](#) reaction rates are low in the absence of catalysts and  
405 require relatively high temperature to occur (i.e. 200-450°C ([Mashkina, 1991](#)), temperatures that  
406 are relevant very close to the fire but unlikely in the [cooled](#) plume). (4) Another possibility is that  
407 a radical intermediate product formed during atmospheric oxidation of DMS (e.g. the  
408 methylthiomethyl radical ( $\text{CH}_3\text{SCH}_2^\bullet$ ) from  $\text{OH}^\bullet$ -driven hydrogen abstraction of DMS (Barnes et  
409 al., 2006)) interacted with CHN and CHON precursors to yield the observed sulfide-containing  
410 CHONS products. However, the concentrations of the methylthiomethyl radical and similar  
411 radicals from other small sulfide precursors would likely be lower than those of other major

412 drivers of in-plume radical chemistry (e.g. O<sub>2</sub>, NO<sub>x</sub>, etc.), thus making this reaction pathway less  
413 likely to contribute.

414         Based on our observations of these sulfide-containing products across flight screens, the  
415 overall timescale for these sulfide-forming reactions was likely approximately 1 hour (or less).  
416 For the literature reactions referenced above, reaction timescales ranged from minutes to hours in  
417 laboratory experiments, but extrapolation to rates in an ambient wildfire plume is uncertain.  
418 Specifically, it is challenging to compare to predicted timescales for the proposed reactions  
419 without knowing the exact structure/identities of the reactants or the possible role of other key  
420 modifying factors in the plume (e.g. aerosol pH, presence of water).

421

## 422 **5 Implications and Conclusions**

423         In this work, we performed the first high resolution tandem mass spectrometry analysis of  
424 an evolving plume from a smoldering boreal forest fire. The results show clear evidence of gas-  
425 phase sulfur-containing emissions from the fire, and an increasing contribution from particle-  
426 phase CHONS compounds with sulfide functional groups as the plume evolved. Together, these  
427 results suggest the emission of gas-phase sulfur-containing compounds from the fire and  
428 subsequent gas- and/or particle-phase chemistry that produced multifunctional sulfide-containing  
429 CHONS compounds.

430         Sulfide functional groups in ambient air have been reported at a range of U.S. locations  
431 from urban inland (1-7% sulfides), urban coastal (5-12% sulfides), and remote forested (7%  
432 sulfides), and on average, sulfides comprised 28% of sulfur-containing functional groups at these  
433 sites (Ditto et al., 2020). However, in past work, 53% of these sulfides were present in CHOS  
434 compounds, while 34% were CHONS, and 13% were CHNS (in contrast to 21%, 71%, and 8%

435 in this study, respectively). Notably, at a Northeastern U.S. coastal site where there were several  
436 pollution events linked to long distance transport of biomass burning smoke during field  
437 sampling (Rogers et al., 2020), 70-90% of sulfides were present in CHONS compounds (Ditto et  
438 al., 2020), similar to the [compound class distribution of](#) sulfides discussed here (Figure 3A).

439         These results, along with past observations, highlight that this type of chemistry and these  
440 types of reaction products may be relevant to other regions where concentrations of nitrogen and  
441 sulfur-containing precursors are high, such as in developing regions, emerging economies, or  
442 megacities where residential biomass burning is common and coincident with extensive use of  
443 sulfur-containing fossil fuels (e.g. coal). CHONS compounds have been reported in similar  
444 regions in past studies (Lin et al., 2012; Pan et al., 2013; Song et al., 2019; Wang et al., 2017a,  
445 2016, 2017b). Their formation is potentially important since the presence of sulfur, oxygen, and  
446 nitrogen [atoms in organic compounds](#) can affect [particle](#) phase state (e.g. solid, semi-solid,  
447 liquid), [and](#) mixing state (e.g. well-mixed, phase-separated) (DeRieux et al., 2018; Ditto et al.,  
448 2019; Van Krevelen and Te Nijenhuis, 2009). These physical properties may influence particles'  
449 chemical reactivity and [overall](#) persistence in the atmosphere, all of which contribute to the  
450 health and environmental impacts that communities and ecosystems experience from OA  
451 exposure. Future work to identify prominent functional groups in CHONS species in regions  
452 with high CHONS concentrations will help elucidate the formation chemistry of these  
453 functionalized compounds and understand and mitigate their associated impacts.

454

455

456

457

458 **Acknowledgments**

459 The authors acknowledge GERSTEL for their collaboration with the TDU 3.5+ used to run the  
460 GC-APCI adsorbent tubes and filters discussed in this study. We thank Environment and Climate  
461 Change Canada and National Research Council technical teams for their help in the construction  
462 and maintenance of cartridge sampling systems, specifically Tak Chan (Environment and  
463 Climate Change Canada) for help collecting samples. We also thank Jo Machesky (Yale) for  
464 help running adsorbent tube samples, Joe Lybik (Yale) for help packing adsorbent tubes, and  
465 Daniel Thompson (Natural Resources Canada) for informative discussion. J.C.D., M.H., T.H-M.,  
466 and D.R.G. acknowledge support from National Science Foundation grant AWD0001666. We  
467 also acknowledge funding from the Air Pollution (AP) program of Environment and Climate  
468 Change Canada. The flights discussed in this study were embedded within a 2018 oil sands  
469 monitoring intensive campaign, and the oil sands monitoring program is acknowledged for  
470 enabling the flights.

471

472 **Author Contributions**

473 J.C.D. ran samples, processed filter data, compiled and interpreted results. M.H. processed  
474 adsorbent tube data. T.H-M. contributed to MS/MS analysis. S.G.M., K.H., J.L., and D.R.G.  
475 collaborated on data interpretation. K.H. collected and processed AMS data. A.L. collected and  
476 processed PTR-ToF-MS data. S.-M.L. designed the aircraft adsorbent tube collection system.  
477 P.L. and J.J.B.W. implemented the wing pod design. P.L. prepared the wing pods for collection  
478 and J.J.B.W. and J.L. collected the adsorbent tube samples. M.J.W. and J.L. designed the filter  
479 collection system. M.J.W. and K.H collected filter samples. S.-M.L., K.H., and J.L. designed the  
480 aircraft sampling study. J.C.D. and D.R.G. wrote the manuscript, with input from all co-authors.

481 **Competing Interests**

482 The authors declare that they have no conflicts of interest.

483

484 **Code and Data Availability**

485 Code and data are available upon request.

486

487 **References**

488 Aas, W., Mortier, A., Bowersox, V., Cherian, R., Faluvegi, G., Fagerli, H., Hand, J., Klimont, Z.,

489 Galy-Lacaux, C., Lehmann, C. M. B., Myhre, C. L., Myhre, G., Olivié, D., Sato, K.,

490 Quaas, J., Rao, P. S. P., Schulz, M., Shindell, D., Skeie, R. B., Stein, A., Takemura, T.,

491 Tsyro, S., Vet, R. and Xu, X.: Global and regional trends of atmospheric sulfur, *Sci. Rep.*,

492 9(1), 1–11, doi:10.1038/s41598-018-37304-0, 2019.

493 Abatzoglou, J. T. and Williams, A. P.: Impact of anthropogenic climate change on wildfire

494 across western US forests, *Proc. Natl. Acad. Sci. U. S. A.*, 113(42), 11770–11775,

495 doi:10.1073/pnas.1607171113, 2016.

496 Ahern, A. T., Robinson, E. S., Tkacik, D. S., Saleh, R., Hatch, L. E., Barsanti, K. C., Stockwell,

497 C. E., Yokelson, R. J., Presto, A. A., Robinson, A. L., Sullivan, R. C. and Donahue, N.

498 M.: Production of Secondary Organic Aerosol During Aging of Biomass Burning Smoke

499 From Fresh Fuels and Its Relationship to VOC Precursors, *J. Geophys. Res. Atmos.*,

500 124(6), 3583–3606, doi:10.1029/2018JD029068, 2019.

501 Akagi, S. K., Yokelson, R. J., Wiedinmyer, C., Alvarado, M. J., Reid, J. S., Karl, T., Crounse, J.

502 D. and Wennberg, P. O.: Emission factors for open and domestic biomass burning for use

503 in atmospheric models, *Atmos. Chem. Phys.*, 11(9), 4039–4072, doi:10.5194/acp-11-

504 4039-2011, 2011.

505 Andreae, M. O.: Emission of trace gases and aerosols from biomass burning – An updated  
506 assessment, *Atmos. Chem. Phys.*, 1–27, doi:10.5194/acp-2019-303, 2019.

507 Canada’s National Forest Inventory, [online] Available from: <https://nfi.nfis.org/en/> (Accessed  
508 18 February 2020), 2020.

509 Barbero, R., Abatzoglou, J. T., Larkin, N. K., Kolden, C. A. and Stocks, B.: Climate change  
510 presents increased potential for very large fires in the contiguous United States, *Int. J.*  
511 *Wildl. Fire*, 24(7), 892–899, doi:10.1071/WF15083, 2015.

512 Barnes, I., Hjorth, J. and Mihalopoulos, N.: Dimethyl sulfide and dimethyl sulfoxide and their  
513 oxidation in the atmosphere, *Chem. Rev.*, 106(3), 940–975, doi:10.1021/cr020529+,  
514 2006.

515 Bertrand, A., Stefenelli, G., Jen, C. N., Pieber, S. M., Bruns, E. A., Ni, H., Temime-Roussel, B.,  
516 Slowik, J. G., Goldstein, A. H., Haddad, I. El, Baltensperger, U., Prévôt, A. S. H.,  
517 Wortham, H. and Marchand, N.: Evolution of the chemical fingerprint of biomass  
518 burning organic aerosol during aging, *Atmos. Chem. Phys.*, 18(10), 7607–7624,  
519 doi:10.5194/acp-18-7607-2018, 2018.

520 Burgos, M. A., Mateos, D., Cachorro, V. E., Toledano, C., de Frutos, A. M., Calle, A.,  
521 Herguedas, A. and Marcos, J. L.: An analysis of high fine aerosol loading episodes in  
522 north-central Spain in the summer 2013 - Impact of Canadian biomass burning episode  
523 and local emissions, *Atmos. Environ.*, doi:10.1016/j.atmosenv.2018.04.024, 2018.

524 Buysse, C. E., Kaulfus, A., Nair, U. and Jaffe, D. A.: Relationships between Particulate Matter,  
525 Ozone, and Nitrogen Oxides during Urban Smoke Events in the Western US, *Environ.*  
526 *Sci. Technol.*, 53(21), 12519–12528, doi:10.1021/acs.est.9b05241, 2019.

527 Colarco, P. R., Schoeberl, M. R., Doddridge, B. G., Marufu, L. T., Torres, O. and Welton, E. J.:  
528 Transport of smoke from Canadian forest fires to the surface near Washington, D.C.:  
529 Injection height, entrainment, and optical properties, *J. Geophys. Res. D Atmos.*, 109(6),  
530 1–12, doi:10.1029/2003JD004248, 2004.

531 Cottle, P., Strawbridge, K. and McKendry, I.: Long-range transport of Siberian wildfire smoke to  
532 British Columbia: Lidar observations and air quality impacts, *Atmos. Environ.*,  
533 doi:10.1016/j.atmosenv.2014.03.005, 2014.

534 Davidian, J.-C. and Kopriva, S.: Regulation of Sulfate Uptake and Assimilation—the Same or  
535 Not the Same?, *Mol. Plant*, 3(2), 314–325, doi:10.1093/MP/SSQ001, 2010.

536 DeRieux, W.-S. W., Li, Y., Lin, P., Laskin, J., Laskin, A., Bertram, A. K., Nizkorodov, S. A. and  
537 Shiraiwa, M.: Predicting the glass transition temperature and viscosity of secondary  
538 organic material using molecular composition, *Atmos. Chem. Phys.*, 18(9), 6331–6351,  
539 doi:10.5194/acp-18-6331-2018, 2018.

540 Ditto, J. C., Barnes, E. B., Khare, P., Takeuchi, M., Joo, T., Bui, A. A. T., Lee-Taylor, J., Eris,  
541 G., Chen, Y., Aumont, B., Jimenez, J. L., Ng, N. L., Griffin, R. J. and Gentner, D. R.: An  
542 omnipresent diversity and variability in the chemical composition of atmospheric  
543 functionalized organic aerosol, *Commun. Chem.*, 1(1), 75, doi:10.1038/s42004-018-  
544 0074-3, 2018.

545 Ditto, J. C., Joo, T., Khare, P., Sheu, R., Takeuchi, M., Chen, Y., Xu, W., Bui, A. A. T., Sun, Y.,  
546 Ng, N. L. and Gentner, D. R.: Effects of Molecular-Level Compositional Variability in  
547 Organic Aerosol on Phase State and Thermodynamic Mixing Behavior, *Environ. Sci.*  
548 *Technol.*, 53(22), 13009–13018, doi:10.1021/acs.est.9b02664, 2019.

549 Ditto, J. C., Joo, T., Slade, J. H., Shepson, P. B., Ng, N. L. and Gentner, D. R.: Nontargeted

550 Tandem Mass Spectrometry Analysis Reveals Diversity and Variability in Aerosol  
551 Functional Groups across Multiple Sites, Seasons, and Times of Day, *Environ. Sci.*  
552 *Technol. Lett.*, 7(2), 60–69, doi:10.1021/acs.estlett.9b00702, 2020.

553 Donahue, N. M., Epstein, S. A., Pandis, S. N. and Robinson, A. L.: A two-dimensional volatility  
554 basis set: 1. organic-aerosol mixing thermodynamics, *Atmos. Chem. Phys.*, 11(7), 3303–  
555 3318, doi:10.5194/acp-11-3303-2011, 2011.

556 Dreessen, J., Sullivan, J. and Delgado, R.: Observations and impacts of transported Canadian  
557 wildfire smoke on ozone and aerosol air quality in the Maryland region on June 9–12,  
558 2015, *J. Air Waste Manag. Assoc.*, 66(9), 842–862,  
559 doi:10.1080/10962247.2016.1161674, 2016.

560 Duporté, G., Parshintsev, J., Barreira, L. M. F., Hartonen, K., Kulmala, M. and Riekkola, M. L.:  
561 Nitrogen-Containing Low Volatile Compounds from Pinonaldehyde-Dimethylamine  
562 Reaction in the Atmosphere: A Laboratory and Field Study, *Environ. Sci. Technol.*,  
563 50(9), 4693–4700, doi:10.1021/acs.est.6b00270, 2016.

564 Duporté, G., Riva, M., Parshintsev, J., Heikkinen, E., Barreira, L. M. F., Myllys, N., Heikkinen,  
565 L., Hartonen, K., Kulmala, M., Ehn, M. and Riekkola, M. L.: Chemical Characterization  
566 of Gas- and Particle-Phase Products from the Ozonolysis of  $\alpha$ -Pinene in the Presence of  
567 Dimethylamine, *Environ. Sci. Technol.*, 51(10), 5602–5610,  
568 doi:10.1021/acs.est.6b06231, 2017.

569 Fenn, M. E., Bytnerowicz, A., Schilling, S. L. and Ross, C. S.: Atmospheric deposition of  
570 nitrogen, sulfur and base cations in jack pine stands in the Athabasca Oil Sands Region,  
571 Alberta, Canada, *Environ. Pollut.*, 196, 497–510, doi:10.1016/j.envpol.2014.08.023,  
572 2015.

573 Forrister, H., Liu, J., Scheuer, E., Dibb, J., Ziemba, L., Thornhill, K. L., Anderson, B., Diskin,  
574 G., Perring, A. E., Schwarz, J. P., Campuzano-Jost, P., Day, D. A., Palm, B. P., Jimenez,  
575 J. L., Nenes, A. and Weber, R. J.: Evolution of brown carbon in wildfire plumes,  
576 *Geophys. Res. Lett.*, 42, 4623–4630, 2015.

577 Forster, C., Wandinger, U., Wotawa, G., James, P., Mattis, I., Althausen, D., Simmonds, P.,  
578 O’Doherty, S., Jennings, S. G., Kleefeld, C., Schneider, J., Trickl, T., Kreipl, S., Jäger, H.  
579 and Stohl, A.: Transport of boreal forest fire emissions from Canada to Europe, J.  
580 *Geophys. Res. Atmos.*, 106(D19), 22887–22906, doi:10.1029/2001JD900115, 2001.

581 Gahan, J. and Schmalenberger, A.: The role of bacteria and mycorrhiza in plant sulfur supply,  
582 *Front. Plant Sci.*, 5(DEC), 1–7, doi:10.3389/fpls.2014.00723, 2014.

583 Garofalo, L. A., Pothier, M. A., Levin, E. J. T., Campos, T., Kreidenweis, S. M. and Farmer, D.  
584 K.: Emission and Evolution of Submicron Organic Aerosol in Smoke from Wildfires in  
585 the Western United States, *ACS Earth Sp. Chem.*, 3(7), 1237–1247,  
586 doi:10.1021/acsearthspacechem.9b00125, 2019.

587 Gilman, J. B., Lerner, B. M., Kuster, W. C., Goldan, P. D., Warneke, C., Veres, P. R., Roberts, J.  
588 M., De Gouw, J. A., Burling, I. R. and Yokelson, R. J.: Biomass burning emissions and  
589 potential air quality impacts of volatile organic compounds and other trace gases from  
590 fuels common in the US, *Atmos. Chem. Phys.*, 15(24), 13915–13938, doi:10.5194/acp-  
591 15-13915-2015, 2015.

592 Hallquist, M., Wenger, J. C., Baltensperger, U., Rudich, Y., Simpson, D., Claeys, M., Dommen,  
593 J., Donahue, N. M., George, C., Goldstein, A. H., Hamilton, J. F., Herrmann, H.,  
594 Hoffmann, T., Iinuma, Y., Jang, M., Jenkin, M. E., Jimenez, J. L., Kiendler-Scharr, A.,  
595 Maenhaut, W., McFiggans, G., Mentel, T. F., Monod, A., Prevot, A. S. H., Seinfeld, J.

596 H., Surratt, J. D., Szmigielski, R. and Wildt, J.: The formation, properties and impact of  
597 secondary organic aerosol: current and emerging issues, *Atmos. Chem. Phys.*, 9(14),  
598 5155–5236, doi:10.5194/acp-9-5155-2009, 2009.

599 Hatch, L. E., Luo, W., Pankow, J. F., Yokelson, R. J., Stockwell, C. E. and Barsanti, K. C.:  
600 Identification and quantification of gaseous organic compounds emitted from biomass  
601 burning using two-dimensional gas chromatography-time-of-flight mass spectrometry,  
602 *Atmos. Chem. Phys.*, 15(4), 1865–1899, doi:10.5194/acp-15-1865-2015, 2015.

603 Hatch, L. E., Rivas-Ubach, A., Jen, C. N., Lipton, M., Goldstein, A. H. and Barsanti, K. C.:  
604 Measurements of I/SVOCs in biomass-burning smoke using solid-phase extraction disks  
605 and two-dimensional gas chromatography, *Atmos. Chem. Phys.*, 18(24), 17801–17817,  
606 doi:10.5194/acp-18-17801-2018, 2018.

607 Hatch, L. E., Jen, C. N., Kreisberg, N. M., Selimovic, V., Yokelson, R. J., Stamatidis, C., York, R.  
608 A., Foster, D., Stephens, S. L., Goldstein, A. H. and Barsanti, K. C.: Highly Speciated  
609 Measurements of Terpenoids Emitted from Laboratory and Mixed-Conifer Forest  
610 Prescribed Fires, *Environ. Sci. Technol.*, 53(16), 9418–9428,  
611 doi:10.1021/acs.est.9b02612, 2019.

612 Hecobian, A., Liu, Z., Hennigan, C. J., Huey, L. G., Jimenez, J. L., Cubison, M. J., Vay, S.,  
613 Diskin, G. S., Sachse, G. W., Wisthaler, A., Mikoviny, T., Weinheimer, A. J., Liao, J.,  
614 Knapp, D. J., Wennberg, P. O., Kürten, A., Crounse, J. D., St. Clair, J., Wang, Y. and  
615 Weber, R. J.: Comparison of chemical characteristics of 495 biomass burning plumes  
616 intercepted by the NASA DC-8 aircraft during the ARCTAS/CARB-2008 field  
617 campaign, *Atmos. Chem. Phys.*, 11(24), 13325–13337, doi:10.5194/acp-11-13325-2011,  
618 2011.

619 Hegg, D. A., Radke, L. F., Hobbs, P. V. and Brock, C. A.: Nitrogen and Sulfur Emissions From  
620 The Burning of Forest Products Near Large Urban Areas, *J. Geophys. Res.*, 92, 701–714,  
621 1987.

622 Hennigan, C. J., Miracolo, M. A., Engelhart, G. J., May, A. A., Presto, A. A., Lee, T., Sullivan,  
623 A. P., McMeeking, G. R., Coe, H., Wold, C. E., Hao, W. M., Gilman, J. B., Kuster, W.  
624 C., De Gouw, J., Schichtel, B. A., Collett, J. L., Kreidenweis, S. M. and Robinson, A. L.:  
625 Chemical and physical transformations of organic aerosol from the photo-oxidation of  
626 open biomass burning emissions in an environmental chamber, *Atmos. Chem. Phys.*,  
627 11(15), 7669–7686, doi:10.5194/acp-11-7669-2011, 2011.

628 Huang, W. Z. and Schoenau, J. J.: Forms, amounts and distribution of carbon, nitrogen,  
629 phosphorus and sulfur in a boreal aspen forest soil, *Can. J. Soil Sci.*, 76(3), 373–385,  
630 doi:10.4141/cjss96-045, 1996.

631 Inuma, Y., Böge, O. and Herrmann, H.: Methyl-nitrocatechols: Atmospheric tracer compounds  
632 for biomass burning secondary organic aerosols, *Environ. Sci. Technol.*, 44(22), 8453–  
633 8459, doi:10.1021/es102938a, 2010.

634 Jencks, W. P. and Lienhard, G. E.: Thiol Addition to the Carbonyl Group. Equilibria and  
635 Kinetics, *J. Am. Chem. Soc.*, 88(17), 3982–3995, doi:10.1021/ja00969a017, 1966.

636 Jiang, H., Frie, A. L., Lavi, A., Chen, J. Y., Zhang, H., Bahreini, R. and Lin, Y. H.: Brown  
637 Carbon Formation from Nighttime Chemistry of Unsaturated Heterocyclic Volatile  
638 Organic Compounds, *Environ. Sci. Technol. Lett.*, 6(3), 184–190,  
639 doi:10.1021/acs.estlett.9b00017, 2019.

640 Jolly, W. M., Cochrane, M. A., Freeborn, P. H., Holden, Z. A., Brown, T. J., Williamson, G. J.  
641 and Bowman, D. M. J. S.: Climate-induced variations in global wildfire danger from

642 1979 to 2013, *Nat. Commun.*, 6(May), 1–11, doi:10.1038/ncomms8537, 2015.

643 Khare, P., Marcotte, A., Sheu, R., Walsh, A. N., Ditto, J. C. and Gentner, D. R.: Advances in  
644 offline approaches for trace measurements of complex organic compound mixtures via  
645 soft ionization and high-resolution tandem mass spectrometry, *J. Chromatogr. A*, 1598,  
646 163–174, doi:10.1016/j.chroma.2019.03.037, 2019.

647 Koss, A. R., Sekimoto, K., Gilman, J. B., Selimovic, V., Coggon, M. M., Zarzana, K. J., Yuan,  
648 B., Lerner, B. M., Brown, S. S., Jimenez, J. L., Krechmer, J., Roberts, J. M., Warneke,  
649 C., Yokelson, R. J. and De Gouw, J.: Non-methane organic gas emissions from biomass  
650 burning: Identification, quantification, and emission factors from PTR-ToF during the  
651 FIREX 2016 laboratory experiment, *Atmos. Chem. Phys.*, 18(5), 3299–3319,  
652 doi:10.5194/acp-18-3299-2018, 2018.

653 Van Krevelen, D. W. and Te Nijenhuis, K.: *Properties of Polymers*, 4th ed., Elsevier,  
654 Amsterdam., 2009.

655 Landis, M. S., Edgerton, E. S., White, E. M., Wentworth, G. R., Sullivan, A. P. and Dillner, A.  
656 M.: The impact of the 2016 Fort McMurray Horse River Wildfire on ambient air  
657 pollution levels in the Athabasca Oil Sands Region, Alberta, Canada, *Sci. Total Environ.*,  
658 618, 1665–1676, doi:10.1016/j.scitotenv.2017.10.008, 2018.

659 Laskin, A., Smith, J. S. and Laskin, J.: Molecular Characterization of Nitrogen-Containing  
660 Organic Compounds in Biomass Burning Aerosols Using High-Resolution Mass  
661 Spectrometry, *Environ. Sci. Technol.*, 43(10), 3764–3771, doi:10.1021/es803456n, 2009.

662 Leustek, T.: Sulfate Metabolism, *Arab. B.*, 1(e0017), 1–16, doi:10.1199/tab.0017, 2002.

663 Li, S. M., Leithead, A., Moussa, S. G., Liggio, J., Moran, M. D., Wang, D., Hayden, K.,  
664 Darlington, A., Gordon, M., Staebler, R., Makar, P. A., Stroud, C. A., McLaren, R., Liu,

665 P. S. K., O'Brien, J., Mittermeier, R. L., Zhang, J., Marson, G., Cober, S. G., Wolde, M.  
666 and Wentzell, J. J. B.: Differences between measured and reported volatile organic  
667 compound emissions from oil sands facilities in Alberta, Canada, *Proc. Natl. Acad. Sci.*  
668 *U. S. A.*, 114(19), E3756–E3765, doi:10.1073/pnas.1617862114, 2017.

669 Li, Y., Pöschl, U. and Shiraiwa, M.: Molecular corridors and parameterizations of volatility in  
670 the chemical evolution of organic aerosols, *Atmos. Chem. Phys.*, 16(5), 3327–3344,  
671 doi:10.5194/acp-16-3327-2016, 2016.

672 Liggio, J., Li, S.-M., Hayden, K., Taha, Y. M., Stroud, C., Darlington, A., Drollette, B. D.,  
673 Gordon, M., Lee, P., Liu, P., Leithead, A., Moussa, S. G., Wang, D., O'Brien, J.,  
674 Mittermeier, R. L., Brook, J. R., Lu, G., Staebler, R. M., Han, Y., Tokarek, T. W.,  
675 Osthoff, H. D., Makar, P. A., Zhang, J., Plata, D. L. and Gentner, D. R.: Oil sands  
676 operations as a large source of secondary organic aerosols, *Nature*, 534,  
677 doi:10.1038/nature17646, 2016.

678 Liggio, J., Moussa, S. G., Wentzell, J., Darlington, A., Liu, P., Leithead, A., Hayden, K., O'Brien,  
679 J., Mittermeier, R. L., Staebler, R., Wolde, M. and Li, S. M.: Understanding the primary  
680 emissions and secondary formation of gaseous organic acids in the oil sands region of  
681 Alberta, Canada, *Atmos. Chem. Phys.*, 17(13), 8411–8427, doi:10.5194/acp-17-8411-  
682 2017, 2017.

683 Lim, C. Y., Hagan, D. H., Coggon, M. M., Koss, A. R., Sekimoto, K., De Gouw, J., Warneke,  
684 C., Cappa, C. D. and Kroll, J. H.: Secondary organic aerosol formation from the  
685 laboratory oxidation of biomass burning emissions, *Atmos. Chem. Phys.*, 19(19), 12797–  
686 12809, doi:10.5194/acp-19-12797-2019, 2019.

687 Lin, P., Yu, J. Z., Engling, G. and Kalberer, M.: Organosulfates in humic-like substance fraction

688 isolated from aerosols at seven locations in East Asia: A study by ultra-high-resolution  
689 mass spectrometry, *Environ. Sci. Technol.*, 46(24), 13118–13127,  
690 doi:10.1021/es303570v, 2012.

691 Lin, P., Fleming, L. T., Nizkorodov, S. A., Laskin, J. and Laskin, A.: Comprehensive Molecular  
692 Characterization of Atmospheric Brown Carbon by High Resolution Mass Spectrometry  
693 with Electrospray and Atmospheric Pressure Photoionization, *Anal. Chem.*, 90(21),  
694 12493–12502, doi:10.1021/acs.analchem.8b02177, 2018.

695 Liu, J. C., Wilson, A., Mickley, L. J., Dominici, F., Ebisu, K., Wang, Y., Sulprizio, M. P., Peng,  
696 R. D., Yue, X., Son, J.-Y., Anderson, G. B. and Bell, M. L.: Wildfire-specific Fine  
697 Particulate Matter and Risk of Hospital Admissions in Urban and Rural Counties,  
698 *Epidemiology*, 28(1), 77–85, doi:10.1111/mec.13536.Application, 2017.

699 Liu, Y., Liggio, J. and Staebler, R.: Reactive uptake of ammonia to secondary organic aerosols:  
700 Kinetics of organonitrogen formation, *Atmos. Chem. Phys.*, 15(23), 13569–13584,  
701 doi:10.5194/acp-15-13569-2015, 2015.

702 Di Lorenzo, R. A., Place, B. K., VandenBoer, T. C. and Young, C. J.: Composition of Size-  
703 Resolved Aged Boreal Fire Aerosols: Brown Carbon, Biomass Burning Tracers, and  
704 Reduced Nitrogen, *ACS Earth Sp. Chem.*, 2(3), 278–285,  
705 doi:10.1021/acsearthspacechem.7b00137, 2018.

706 Lowe, A. B.: Thiol-ene “click” reactions and recent applications in polymer and materials  
707 synthesis, *Polym. Chem.*, 1(1), 17–36, doi:10.1039/b9py00216b, 2010.

708 Makar, P. A., Akingunola, A., Aherne, J., Cole, A. S., Aklilu, Y. A., Zhang, J., Wong, I.,  
709 Hayden, K., Li, S. M., Kirk, J., Scott, K., Moran, M. D., Robichaud, A., Cathcart, H.,  
710 Baratzedah, P., Pabla, B., Cheung, P., Zheng, Q. and Jeffries, D. S.: Estimates of

711 exceedances of critical loads for acidifying deposition in Alberta and Saskatchewan,  
712 *Atmos. Chem. Phys.*, 18(13), 9897–9927, doi:10.5194/acp-18-9897-2018, 2018.

713 Mashkina, A. V.: Catalytic Synthesis Of Sulfides Sulfoxides and Sulfones, *Sulfur reports*, 10(4),  
714 279–388, doi:10.1080/01961779108048759, 1991.

715 McLinden, C. A., Fioletov, V., Krotkov, N. A., Li, C., Boersma, K. F. and Adams, C.: A Decade  
716 of Change in NO<sub>2</sub> and SO<sub>2</sub> over the Canadian Oil Sands As Seen from Space, *Environ.*  
717 *Sci. Technol.*, 50(1), 331–337, doi:10.1021/acs.est.5b04985, 2016.

718 Meng, F. R., Bourque, C. P. A., Belczewski, R. F., Whitney, N. J. and Arp, P. A.: Foliage  
719 responses of spruce trees to long-term low-grade sulfur dioxide deposition, *Environ.*  
720 *Pollut.*, 90(2), 143–152, doi:10.1016/0269-7491(94)00101-I, 1995.

721 Murphy, B. N., Donahue, N. M., Robinson, A. L. and Pandis, S. N.: A naming convention for  
722 atmospheric organic aerosol, *Atmos. Chem. Phys.*, 14(11), 5825–5839, doi:10.5194/acp-  
723 14-5825-2014, 2014.

724 Nozière, B., Kalberer, M., Claeys, M., Allan, J., D’Anna, B., Decesari, S., Finessi, E., Glasius,  
725 M., Grgić, I., Hamilton, J. F., Hoffmann, T., Iinuma, Y., Jaoui, M., Kahnt, A., Kampf, C.  
726 J., Kourtchev, I., Maenhaut, W., Marsden, N., Saarikoski, S., Schnelle-Kreis, J., Surratt,  
727 J. D., Szidat, S., Szmigielski, R. and Wisthaler, A.: The Molecular Identification of  
728 Organic Compounds in the Atmosphere: State of the Art and Challenges, *Chem. Rev.*,  
729 115(10), 3919–3983, doi:10.1021/cr5003485, 2015.

730 Nyborg, M., Solberg, E. D., Malhi, S. S., Takyi, S., Yeung, P. and Chaudhry, M.: Deposition of  
731 anthropogenic sulphur dioxide on soils and resulting soil acidification, *Plant-Soil Interact.*  
732 *Low pH*, 147–156, doi:10.1007/978-94-011-3438-5\_16, 1991.

733 Onda, Y.: Oxidative protein-folding systems in plant cells, *Int. J. Cell Biol.*, 2013,

734 doi:10.1155/2013/585431, 2013.

735 Pan, Y. P., Wang, Y. S., Tang, G. Q. and Wu, D.: Spatial distribution and temporal variations of  
736 atmospheric sulfur deposition in Northern China: Insights into the potential acidification  
737 risks, *Atmos. Chem. Phys.*, 13(3), 1675–1688, doi:10.5194/acp-13-1675-2013, 2013.

738 Reid, C. E., Brauer, M., Johnston, F. H., Jerrett, M., Balmes, J. R. and Elliott, C. T.: Critical  
739 review of health impacts of wildfire smoke exposure, *Environ. Health Perspect.*, 124(9),  
740 1334–1343, doi:10.1289/ehp.1409277, 2016.

741 Rogers, H. M., Ditto, J. C. and Gentner, D. R.: Evidence for impacts on surface-level air quality  
742 in the northeastern US from long-distance transport of smoke from North American fires  
743 during the Long Island Sound Tropospheric Ozone Study (LISTOS) 2018, *Atmos. Chem.*  
744 *Phys.*, 20(2), 671–682, doi:10.5194/acp-20-671-2020, 2020.

745 Sekimoto, K., Koss, A. R., Gilman, J. B., Selimovic, V., Coggon, M. M., Zarzana, K. J., Yuan,  
746 B., Lerner, B. M., Brown, S. S., Warneke, C., Yokelson, R. J., Roberts, J. M. and De  
747 Gouw, J.: High-and low-temperature pyrolysis profiles describe volatile organic  
748 compound emissions from western US wildfire fuels, *Atmos. Chem. Phys.*, 18(13),  
749 9263–9281, doi:10.5194/acp-18-9263-2018, 2018.

750 Sengupta, D., Samburova, V., Bhattarai, C., Kirillova, E., Mazzoleni, L., Iaukea-Lum, M., Watts,  
751 A., Moosmüller, H. and Khlystov, A.: Light absorption by polar and non-polar aerosol  
752 compounds from laboratory biomass combustion, *Atmos. Chem. Phys.*, 18(15), 10849–  
753 10867, doi:10.5194/acp-18-10849-2018, 2018.

754 Sheu, R., Marcotte, A., Khare, P., Charan, S., Ditto, J. C. and Gentner, D. R.: Advances in  
755 offline approaches for chemically speciated measurements of trace gas-phase organic  
756 compounds via adsorbent tubes in an integrated sampling-to-analysis system, *J.*

757 Chromatogr. A, 1575, 80–90, doi:10.1016/j.chroma.2018.09.014, 2018.

758 Song, J., Li, M., Fan, X., Zou, C., Zhu, M., Jiang, B., Yu, Z., Jia, W., Liao, Y. and Peng, P.:  
759 Molecular Characterization of Water- And Methanol-Soluble Organic Compounds  
760 Emitted from Residential Coal Combustion Using Ultrahigh-Resolution Electrospray  
761 Ionization Fourier Transform Ion Cyclotron Resonance Mass Spectrometry, Environ. Sci.  
762 Technol., 53(23), 13607–13617, doi:10.1021/acs.est.9b04331, 2019.

763 Updyke, K. M., Nguyen, T. B. and Nizkorodov, S. A.: Formation of brown carbon via reactions  
764 of ammonia with secondary organic aerosols from biogenic and anthropogenic  
765 precursors, Atmos. Environ., 63, 22–31, doi:10.1016/j.atmosenv.2012.09.012, 2012.

766 Val Martín, M., Honrath, R. E., Owen, R. C., Pfister, G., Fialho, P. and Barata, F.: Significant  
767 enhancements of nitrogen oxides, black carbon, and ozone in the North Atlantic lower  
768 free troposphere resulting from North American boreal wildfires, J. Geophys. Res.  
769 Atmos., 111(23), 1–17, doi:10.1029/2006JD007530, 2006.

770 Vicente, A., Alves, C., Calvo, A. I., Fernandes, A. P., Nunes, T., Monteiro, C., Almeida, S. M.  
771 and Pio, C.: Emission factors and detailed chemical composition of smoke particles from  
772 the 2010 wildfire season, Atmos. Environ., doi:10.1016/j.atmosenv.2013.01.062, 2013.

773 Wang, X., Wang, H., Jing, H., Wang, W. N., Cui, W., Williams, B. J. and Biswas, P.: Formation  
774 of Nitrogen-Containing Organic Aerosol during Combustion of High-Sulfur-Content  
775 Coal, Energy and Fuels, 31(12), 14161–14168, doi:10.1021/acs.energyfuels.7b02273,  
776 2017a.

777 Wang, X. K., Rossignol, S., Ma, Y., Yao, L., Wang, M. Y., Chen, J. M., George, C. and Wang,  
778 L.: Molecular characterization of atmospheric particulate organosulfates in three  
779 megacities at the middle and lower reaches of the Yangtze River, Atmos. Chem. Phys.,

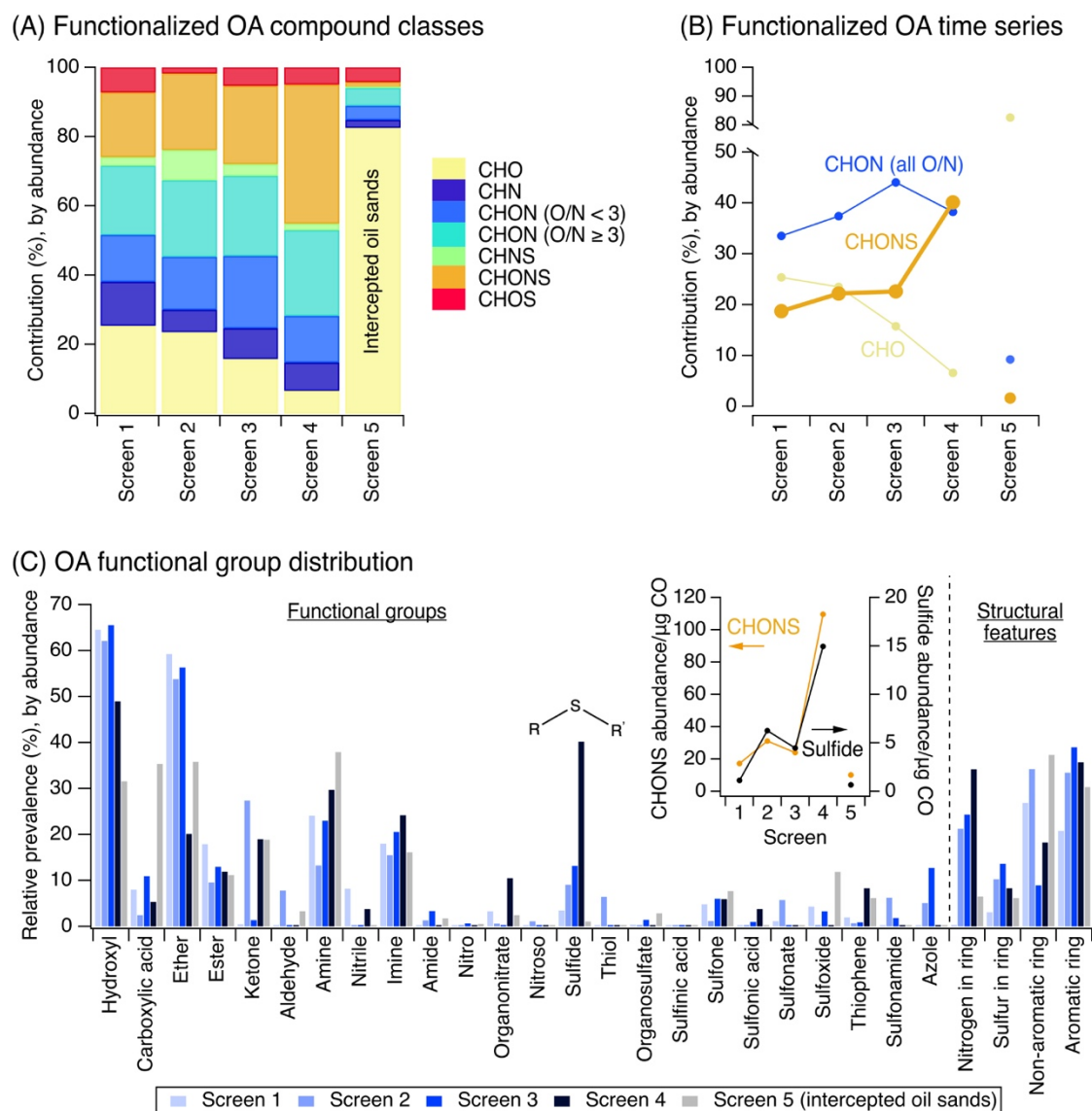
780 16(4), 2285–2298, doi:10.5194/acp-16-2285-2016, 2016.

781 Wang, X. K., Hayeck, N., Brüggemann, M., Yao, L., Chen, H., Zhang, C., Emmelin, C., Chen,  
782 J., George, C. and Wang, L.: Chemical Characteristics of Organic Aerosols in Shanghai:  
783 A Study by Ultrahigh-Performance Liquid Chromatography Coupled With Orbitrap Mass  
784 Spectrometry, *J. Geophys. Res. Atmos.*, 122(21), 11,703–11,722,  
785 doi:10.1002/2017JD026930, 2017b.

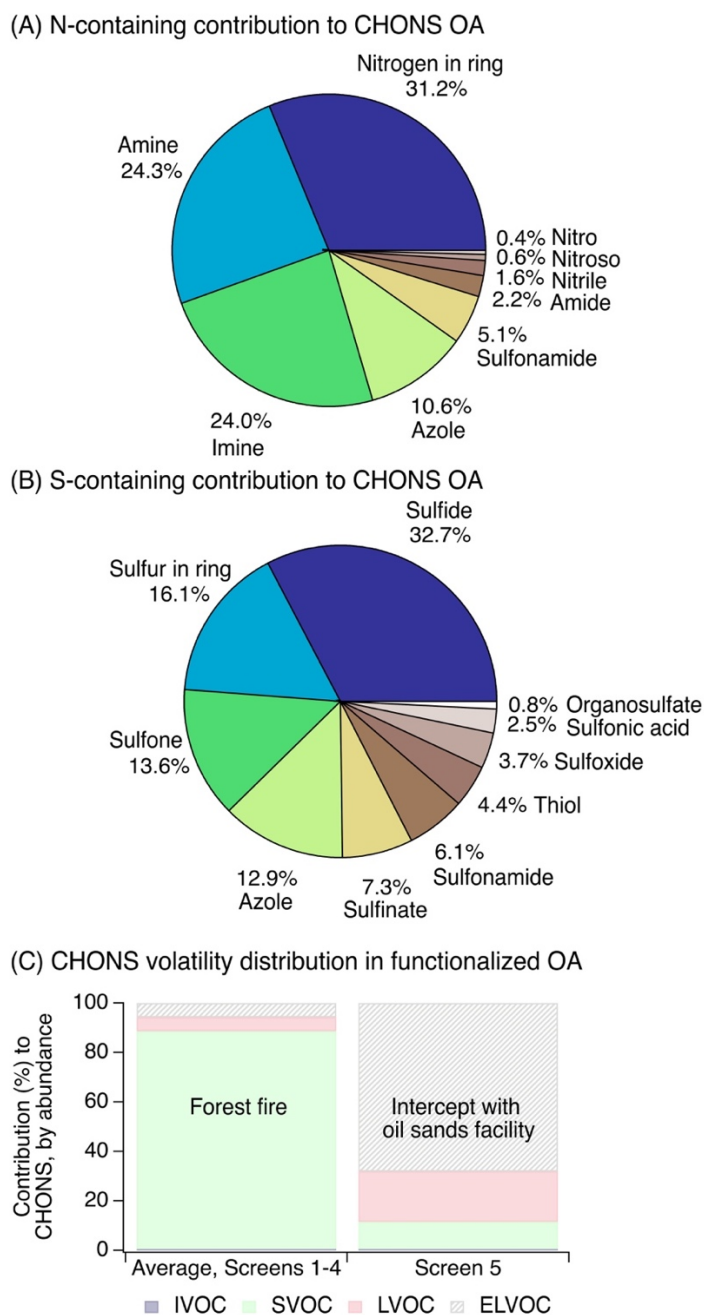
786 Ward, D. E.: Factors Influencing the Emissions of Gases and Particulate Matter from Biomass  
787 Burning, in *Fire in the Tropical Biota: Ecosystem Processes and Global Challenges*, pp.  
788 418–436., 1990.

789 Wong, J. P. S., Tsagkaraki, M., Tsiodra, I., Mihalopoulos, N., Violaki, K., Kanakidou, M.,  
790 Sciare, J., Nenes, A. and Weber, R. J.: Effects of Atmospheric Processing on the  
791 Oxidative Potential of Biomass Burning Organic Aerosols, *Environ. Sci. Technol.*,  
792 53(12), 6747–6756, doi:10.1021/acs.est.9b01034, 2019.

793 Yokelson, R. J., Burling, I. R., Gilman, J. B., Warneke, C., Stockwell, C. E., De Gouw, J., Akagi,  
794 S. K., Urbanski, S. P., Veres, P., Roberts, J. M., Kuster, W. C., Reardon, J., Griffith, D.  
795 W. T., Johnson, T. J., Hosseini, S., Miller, J. W., Cocker, D. R., Jung, H. and Weise, D.  
796 R.: Coupling field and laboratory measurements to estimate the emission factors of  
797 identified and unidentified trace gases for prescribed fires, *Atmos. Chem. Phys.*, 13(1),  
798 89–116, doi:10.5194/acp-13-89-2013, 2013.

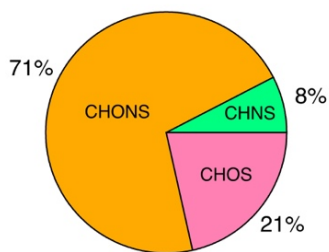


799 **Figure 1.** (A) The compound class distribution of functionalized OA (from non-targeted LC-  
800 ESI-MS) weighted by ion abundance, shown as percent contribution of each compound class to  
801 the total compound abundance measured by LC-ESI-MS. (B) Percent contribution of CHO,  
802 CHON, and CHONS compound classes in functionalized OA as a function of plume age. CHON  
803 compounds in panel B are summed across all O/N ratios. (C) Functional groups and structural  
804 features present in measured functionalized OA (from non-targeted LC-ESI-MS/MS). The  
805 sulfide functional group is shown here for emphasis, and will be the subject of subsequent  
806 analyses. The inset in panel C shows the absolute CHONS ion abundance normalized by CO  
807 mass (orange trace, left y-axis) and the absolute sulfide ion abundance normalized by CO mass  
808 (black trace, right y-axis). Full CO-adjusted compound class and functional group  
809 abundance data are shown in Figures S5-S6. For panels A-C, results tabulated by occurrence are also  
810 in Figure S5-S6.

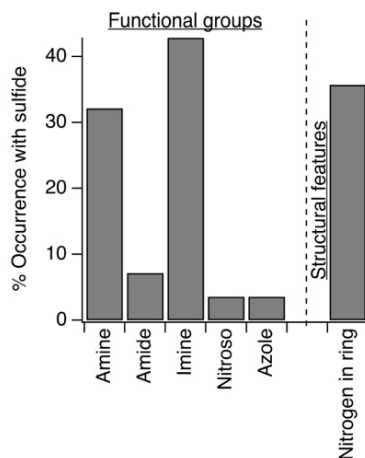


811 **Figure 2.** (A) The distribution of nitrogen-containing functional groups to particle-phase  
 812 CHONS compounds (organonitrates are excluded here due to challenges with their identification  
 813 using SIRIUS with CSI:FingerID, but contributed minimally to CHONS, Supporting Information  
 814 S3). (B) The distribution of sulfur-containing groups to particle-phase CHONS compounds.  
 815 For panels A-B, data are averaged across screens 1-4, with individual screens shown in Figure  
 816 S7A. (C) Volatility distribution of particle-phase CHONS species. These volatility data were  
 817 averaged across screens 1-4, and individual screens are shown in Figure S8. Volatility was  
 818 estimated with the parameterization in Li et al. (Li et al., 2016) and grouped according to  
 819 volatility bins in Donahue et al. (Donahue et al., 2011).

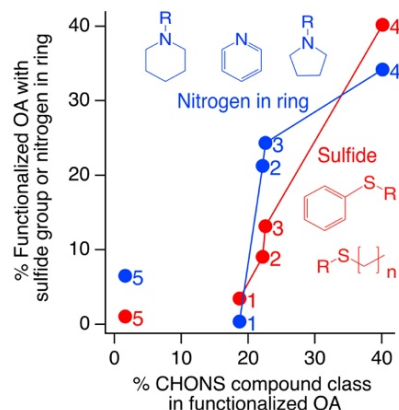
(A) Compound class of sulfides in functionalized OA



(B) N-groups co-occurring with sulfides in functionalized OA

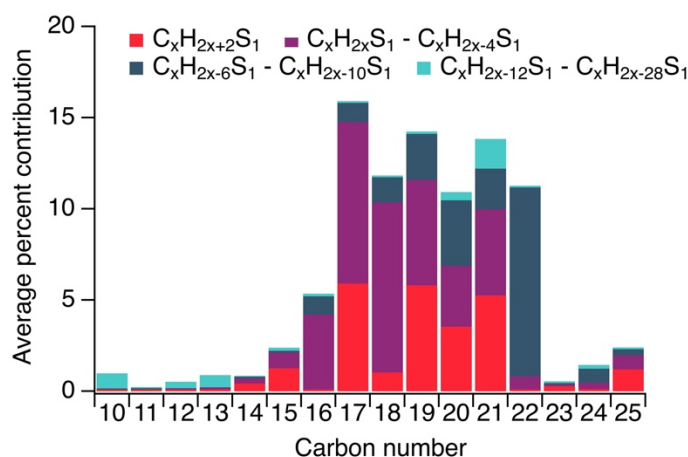


(C) Evolution with CHONS OA

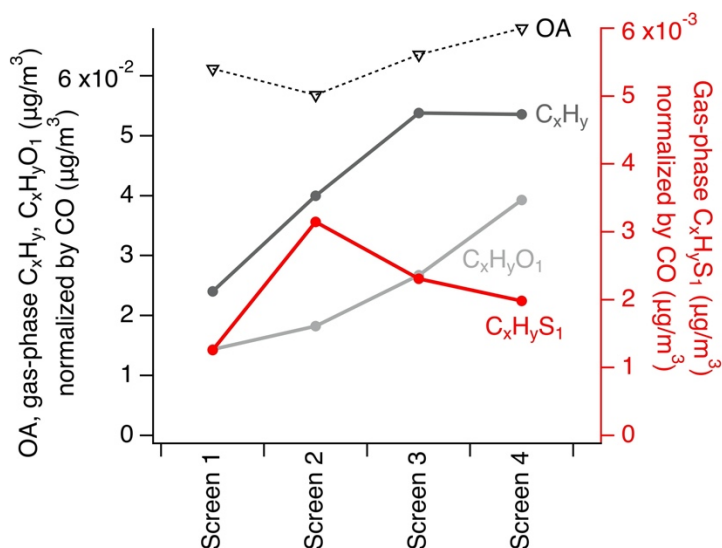


820 **Figure 3.** (A) Compound class distribution of sulfide groups: 71% of sulfide functional groups  
821 observed (weighted by ion abundance) were present in CHONS compounds. (B) Co-occurrence  
822 of sulfides and nitrogen-containing groups. Data shown in panels A-B are cumulative across  
823 compounds in screens 1-4. (C) The relative contribution of sulfides and cyclic nitrogen groups to  
824 all functionalized OA increased together with the increasing contribution of CHONS  
825 compounds. The other functional groups in panel B showed no relationship with the increase in  
826 CHONS (Figure S7B). Structures represent examples of commonly observed sulfide and cyclic  
827 nitrogen substructures from SIRIUS and CSI:FingerID (Supporting Information S3), where ring  
828 structures associated with nitrogen heteroatoms were free standing, adjacent to other rings,  
829 and/or contained additional attached functional groups.

(A) Average gas-phase  $C_xH_yS_1$  distribution



(B) Gas-phase and AMS OA concentrations normalized by CO



830 **Figure 4.** (A) The average  $C_xH_yS_1$  distribution from targeted GC-APCI-MS across all gas-phase  
831 adsorbent tube samples from screens 1-4 (see Figure S10 for individual  $C_xH_yS_1$  screens, and  
832 Figure S13 for  $C_xH_y$ ). (B) Concentrations of gas-phase  $C_xH_y$ ,  $C_xH_yO_1$ ,  $C_xH_yS_1$  from targeted GC-  
833 APCI-MS analysis of adsorbent tubes, shown with total OA from AMS, all corrected for dilution  
834 using carbon monoxide measurements (see Figure S12A for non-normalized concentrations).  
835 Data in panel B are averaged over low and high altitude adsorbent tube samples.